Atmos. Meas. Tech., 6, 565–584, 2013
www.atmos-meas-tech.net/6/565/2013/
doi:10.5194/amt-6-565-2013

Atmospheric Measurement Techniques
Open Access

Improvements to the retrieval of tropospheric NO_2 from satellite – stratospheric correction using SCIAMACHY limb/nadir matching and comparison to Oslo CTM2 simulations

A. Hilboll[1], **A. Richter**[1], **A. Rozanov**[1], **Ø. Hodnebrog**[2,*], **A. Heckel**[3,1], **S. Solberg**[4], **F. Stordal**[2], **and J. P. Burrows**[1]

[1]Institute of Environmental Physics, University of Bremen, P.O. Box 330 440, 28334 Bremen, Germany
[2]University of Oslo, Oslo, Norway
[3]Department of Geography, Swansea University, Swansea, UK
[4]Norwegian Institute for Air Research, Kjeller, Norway
[*]now at: Center for International Climate and Environmental Research-Oslo (CICERO), Oslo, Norway

Correspondence to: A. Hilboll (hilboll@iup.physik.uni-bremen.de)

Received: 12 June 2012 – Published in Atmos. Meas. Tech. Discuss.: 23 July 2012
Revised: 6 December 2012 – Accepted: 18 January 2013 – Published: 1 March 2013

Abstract. Satellite measurements of atmospheric trace gases have proved to be an invaluable tool for monitoring the Earth system. When these measurements are to be used for assessing tropospheric emissions and pollution, as for example in the case of nadir measurements of nitrogen dioxide (NO_2), it is necessary to separate the stratospheric from the tropospheric signal.

The SCIAMACHY instrument offers the unique opportunity to combine its measurements in limb- and nadir-viewing geometries into a tropospheric data product, using the limb measurements of the stratospheric NO_2 abundances to correct the nadir measurements' total columns.

In this manuscript, we present a novel approach to limb/nadir matching, calculating one stratospheric NO_2 value from limb measurements for every single nadir measurement, abandoning global coverage for the sake of spatial accuracy. For comparison, modelled stratospheric NO_2 columns from the Oslo CTM2 are also evaluated for stratospheric correction.

Our study shows that stratospheric NO_2 columns from SCIAMACHY limb measurements very well reflect stratospheric conditions. The zonal variability of the stratospheric NO_2 field is captured by our matching algorithm, and the quality of the resulting tropospheric NO_2 columns improves considerably. Both stratospheric datasets need to be adjusted to the level of the nadir measurements, because a time- and latitude-dependent bias to the measured nadir columns can be observed over clean regions. After this offset is removed, the two datasets agree remarkably well, and both stratospheric correction methods provide a significant improvement to the retrieval of tropospheric NO_2 columns from the SCIAMACHY instrument.

1 Introduction

For several decades, satellite-based instruments have been used to investigate the chemical composition of the Earth's atmosphere. Since the mid-1990s, the Global Ozone Monitoring Experiment (GOME, Burrows et al., 1999), the SCanning Imaging Absorption spectroMeter for Atmospheric CHartographY (SCIAMACHY, Bovensmann et al., 1999; Burrows et al., 1995, and references therein), the Ozone Monitoring Instrument (OMI, Levelt et al., 2006), and GOME's successor GOME-2 (Callies et al., 2000) have been launched in the class of nadir-viewing UV/visible instruments.

They all measure the solar radiation scattered in the atmosphere and reflected by the Earth's surface in the UV/visible spectral region. While most of these instruments were originally designed to investigate the evolution of stratospheric ozone, their measurements allow for the analysis of a broad range of atmospheric constituents. One possible retrieval method is differential optical absorption spectroscopy (DOAS), a method based on the Beer–Lambert law which yields the quantity total slant column density (SCD_{tot}), the concentration of a specific absorber integrated along the effective light path through the atmosphere. These slant columns are then converted into vertical column densities (VCD) using so-called air mass factors (AMF), derived from radiative transfer calculations. A thorough description of the DOAS technique can be found in Platt and Stutz (2008), and an overview on the retrieval tropospheric of trace gases from space is given in Burrows et al. (2011).

Several trace gases have been analysed with the DOAS technique, e.g. nitrogen dioxide (NO_2; among others: Richter and Burrows, 2002; Leue et al., 2001; Martin et al., 2002; Boersma et al., 2007), formaldehyde (Wittrock, 2006; de Smedt et al., 2010), bromine monoxide (Richter et al., 1998; Platt and Wagner, 1998; Chance, 1998), and iodine monoxide (Schönhardt et al., 2008). In this study, we focus on the retrieval of tropospheric NO_2. This particular trace gas is mainly produced by anthropogenic activities; other sources include lightning (Beirle et al., 2004), biomass burning (Lee et al., 1997), and soil processes (Williams et al., 1992; Bertram et al., 2005). NO_2 plays a key role in tropospheric (as an important ozone precursor) as well as in stratospheric (being involved in ozone destruction) chemistry (Crutzen, 1979; Brasseur and Solomon, 2005). In both altitude regions, NO_2 quickly interchanges with nitric oxide (NO), which is why the sum of the two molecules is often referred to as NO_x. While anthropogenic emissions of NO cannot be directly monitored from space, the relatively short lifetime of the NO_2 molecule in the troposphere (between several hours and a few days, depending on atmospheric conditions) allows for the investigation of the spatiotemporal variability of NO_x emissions. Nitrous oxide (N_2O), which gets emitted at the surface mainly by microbial activity in soils, has a lifetime long enough to facilitate its transport into the stratosphere. There it reacts with an excited singlet D oxygen atom to produce two NO molecules (Brasseur and Solomon, 2005), forming the main source of stratospheric NO_x.

Since the DOAS method yields the trace gas' total slant column density, the investigation of its tropospheric abundance needs additional information to separate the signal into its tropospheric and stratospheric components. A widely used method is the relatively simple reference sector method, in which the measurements taken in a region over the Pacific Ocean are assumed to include no tropospheric contribution (Richter and Burrows, 2002; Martin et al., 2002). The average of these "clean" measurements is then subtracted from all measurements of the same day latitude-wise. Due to the low zonal variability of stratospheric NO_2 and the satellites' sun-synchronous orbit, the method often yields reasonable results. However, this approximation sometimes leads to unphysical negative tropospheric column densities (SCD_{trop}), e.g. in areas affected by the polar vortex (see e.g. Fig. 17, top). This is the most visible sign that the assumption of zonal homogeneity is not always correct and shows the need to improve the quality of stratospheric NO_2 fields, especially of their fine-scaled structures (Richter and Burrows, 2002; Boersma et al., 2004). Therefore, several other stratospheric correction schemes have been used to estimate the vertical stratospheric NO_2 columns (VCD_{strat}), namely (a) elaborating on the reference sector method by selecting a range of areas classified as unpolluted, (b) using a global chemistry and transport model (CTM), and (c) making use of independent measurements.

The earliest improvements with respect to the reference sector method have been suggested by Leue et al. (2001) and Wenig et al. (2004). In these studies, several regions around the globe have been classified as unpolluted, and a global field of VCD_{strat} has been interpolated from the measurements over these regions. Later, Bucsela et al. (2006) further refined this method by using a wave-2 fit along zonal bands to estimate stratospheric NO_2 column densities over polluted regions. However, both methods suffer from the same drawback by requiring the definition of unpolluted regions, which can lead to too high estimates for VCD_{strat} in the case of a smooth tropospheric background signal, e.g. from soil emissions, biomass burning, and long-range transport.

Regarding correction scheme (b), a number of different approaches have been used to estimate stratospheric NO_2 columns. Stratospheric column densities from the SLIMCAT model adjusted to the measurements over the Pacific have been used by Richter et al. (2005), while Boersma et al. (2007) assimilated the satellite's NO_2 measurements over unpolluted regions into the TM4 model. This has the advantage of combining the absolute values from the measurements with the spatial distribution of the model. In this study, we investigate the use of stratospheric NO_2 columns from the Oslo CTM2 model, as described in Sect. 2.4.

As for correction scheme (c), SCIAMACHY is the first instrument to combine limb- and nadir-mode measurements of approximately the same air mass, taken within 15 min of each other (Bovensmann et al., 1999). This offers the unique opportunity to use independent measurements done by the same instrument to investigate the stratospheric contribution to the total signal. In nadir geometry, SCIAMACHY looks down towards the Earth's surface, and it measures total trace gas columns. In limb geometry, however, the instrument operates forward-looking and scans the atmosphere from the surface to a tangent height of 92 km (Gottwald and Bovensmann, 2011), thereby allowing for the retrieval of vertical absorber profiles using scattered light only. This limb/nadir matching has been exemplarily investigated in several studies (Sierk et al., 2006; Sioris et al., 2004). Beirle et al. (2010) have gone further and created a standard data product of stratospheric NO_2 for the extraction of the tropospheric NO_2 field by calculating a smoothed and interpolated global field from SCIAMACHY's limb-mode measurements.

In the present study, we use the SCIAMACHY limb-mode measurements in a different way, avoiding the smoothing and (most of the) interpolating steps taken by Beirle et al. (2010) by calculating VCD_{strat} for the locations of SCIAMACHY's nadir-mode measurements only. This is important because stratospheric NO_2 columns can show large day-to-day dynamical effects, especially in regions affected by the polar vortex, as shown by Dirksen et al. (2011). While this procedure, which is detailed in Sect. 3.2, yields the best possible matching of nadir and limb measurements, the stratospheric data product does not give daily global coverage, which means that this correction scheme is only suitable for SCIAMACHY measurements. The algorithm is tailored to provide a full dataset of tropospheric NO_2 from all available SCIAMACHY measurements from 2002 until the end of SCIAMACHY operations in 2012. Application of SCIAMACHY limb measurements for stratospheric correction is compared to the use of model simulations carried out with the Oslo CTM2 model, and the simple reference sector method. This comparison is based on evaluation of (a) latitudinal and longitudinal variability of the derived stratospheric NO_2 fields and (b) the resulting fields of tropospheric NO_2.

2 Datasets used in this study

2.1 SCD_{tot} from SCIAMACHY nadir measurements

To calculate total slant column densities from the spectra measured by SCIAMACHY, the NO_2 absorption averaged over all light paths contributing to the signal is determined using DOAS (Platt and Stutz, 2008) in the 425–450 nm wavelength region (Richter and Burrows, 2002). Additionally to NO_2, the trace gases O_3, O_4, and H_2O are included in the fitting procedure. The NO_2 and O_3 absorption cross sections used in the fitting procedure have been measured at 243 K (Bogumil et al., 2003). Furthermore, a synthetic Ring spectrum (Vountas et al., 1998), an undersampling correction (Chance, 1998), and a calibration function accounting for the polarisation dependency of the SCIAMACHY spectral response are included in the fit. A polynomial of degree 3 is used to account for low frequency variations of the optical density, for example from scattering.

2.2 SCIAMACHY limb profile retrieval

The limb-mode measurements made by SCIAMACHY are the most elaborate global assessment of stratospheric NO_2 available today. The instrument operates forward-looking and scans the atmosphere from the surface to a tangent height of 92 km (Gottwald and Bovensmann, 2011), thereby allowing the retrieval of vertical absorber profiles using scattered light only. The ground scene of a limb scan is defined by the geolocation of the line-of-sight tangent point at the start and end of the state. In every limb state, four distinct vertical profiles are recorded, each covering a ground area 240 km wide. Due to the elevation steps executed by the instrument, the tangent point of the line-of-sight moves slightly towards the spacecraft as the platform moves along the orbit. The satellite's movement around the Earth thus leads to a rather narrow appearance of the along-track extent of the limb pixels (Gottwald and Bovensmann, 2011). About 100 limb NO_2 profiles are taken by SCIAMACHY each orbit.

In this study, we use the NO_2 concentration profiles from the IUP Bremen scientific retrieval, version 3.1. The software package SCIATRAN (Rozanov et al., 2005b) is used for the retrieval of these absorber concentrations. The retrieval is performed in the 420–470 nm wavelength range, after all measured limb radiances have been normalized with respect to the radiance at tangent height 43 km in order to eliminate spectral features emerging from solar Fraunhofer lines. Stratospheric absorber concentrations are then inverted from the measured spectra using the information operator approach (Bauer et al., 2012). Apart from NO_2, O_3 and O_4 are included in the forward model, and the temperature dependence of the cross sections is considered using ECMWF (European Centre for Medium-Range Weather Forecasting) data. The retrieved profiles yield NO_2 concentrations for tangent heights from $\approx$ 10–40 km, with a vertical sampling of 1 km and a vertical resolution of 3–5 km. This dataset has been validated by Bauer et al. (2012).

For those measurements where the tropopause lies below the lower boundary of the retrieved SCIAMACHY limb profiles, the profiles were extended down towards the tropopause by NO_2 concentration profiles derived from a monthly climatology created from the Oslo CTM2 model run (see Sect. 2.4).

2.3 Tropopause altitude

The tropopause height was computed on a latitude/longitude grid of 1.5° resolution, using the ECMWF ERA-Interim reanalysis (Dee et al., 2011). The location of the tropopause was obtained by applying both dynamical (potential vorticity) and thermal (lapse rate) definitions, following an approach similar to the one discussed in Hoinka (1998). The combination of the dynamical and thermal criteria enables a clear definition of the boundary between the troposphere and the stratosphere. For the tropics we applied the thermal criterion and from the mid-latitudes to the poles we applied the dynamical criterion using a potential vorticity of 3 PVU ($1\,\mathrm{PVU} = 10^{-6}\,\mathrm{km^2\,s^{-1}\,kg^{-1}}$). In the transition region between the two regimes, both criteria were used and weighted with the distance from the regime boundaries. This method is further described in Ebojie et al. (2013).

2.4 Oslo CTM2 simulations

Since appropriate profile measurements are not available, model simulations are used to obtain quantities for verification purposes. The NO_2 vertical profiles and tropospheric column NO_2 values have been validated independently (e.g. Bauer et al., 2012; Heue et al., 2005; Richter et al., 2004). Additionally, model simulations have to be used to estimate the tropospheric background signal (see Sect. 3.5).

In this study, we use NO_2 columns modelled by the Oslo CTM2 model (Søvde et al., 2008). The model is driven by meteorological data from the ECMWF Integrated Forecast System (IFS) model, and has been run with both tropospheric (Berntsen and Isaksen, 1997) and stratospheric (Stordal et al., 1985) chemistry for the period 1997–2007, whereof the latter ten years have been used in the analysis (1997 was considered as spin-up). It extends from the surface to 0.1 hPa in 60 vertical layers, and a horizontal resolution of Gaussian T42 ($2.8125° \times 2.8125°$) has been used. Anthropogenic emissions are taken from the MACCity inventory (Granier et al., 2011), while biogenic emissions are from POET (Granier et al., 2005). Biomass burning emissions are from RETRO (Schultz et al., 2008) for 1997–2000 and from GFEDv2 (van der Werf et al., 2006) for the remaining period. Lightning emissions are based on Price et al. (1997) and redistributed according to lightning frequencies; the procedure is described in detail in Søvde et al. (2008). Advection in Oslo CTM2 is done using the second order moment scheme (Prather, 1986), convection is based on the Tiedtke mass flux parametrisation (Tiedtke, 1989), and boundary layer mixing is treated according to the Holtslag K-profile method (Holtslag et al., 1990). The quasi-steady-state approximation (Hesstvedt et al., 1978) is used for the numerical solution in the chemistry scheme, and photo-dissociation is done online using the FAST-J2 method (Wild et al., 2000; Bian and Prather, 2002).

Vertical stratospheric NO_2 columns are calculated by integrating the modelled concentrations from the tropopause to the top of the modelled atmosphere at 0.1 hPa. For this purpose, the tropopause height is fixed to the layer interface that is closest to the "real" tropopause altitude calculated using the 2.5 PVU criterion. Compared to the hybrid criterion used in the calculation of measured stratospheric columns (see Sect. 2.3), this only leads to minor differences due to the strong vertical gradient in the PV field near the tropopause.

3 Stratospheric correction algorithm

This study concentrates on converting total to tropospheric slant columns by using stratospheric NO_2 profiles retrieved from SCIAMACHY limb measurements as described in Sect. 2.2. First, as the SCIAMCHY limb retrieval is sensitive down to approximately 11 km, the stratospheric NO_2 profiles must be extrapolated downward to the tropopause. The resulting vertical profiles are then integrated into VCD_{strat} (Sect. 3.1). In a next step, the limb measurements are geographically matched to the nadir measurements (Sect. 3.2). While the limb pixels' small extent probably does not optimally reproduce the actual volume observed by the instrument, the definition via the line-of-sight tangent point is still the most plausible description, not needing computationally expensive 3-D radiative transfer calculations (Pukïte et al., 2010). The small pixel sizes in along-track direction lead

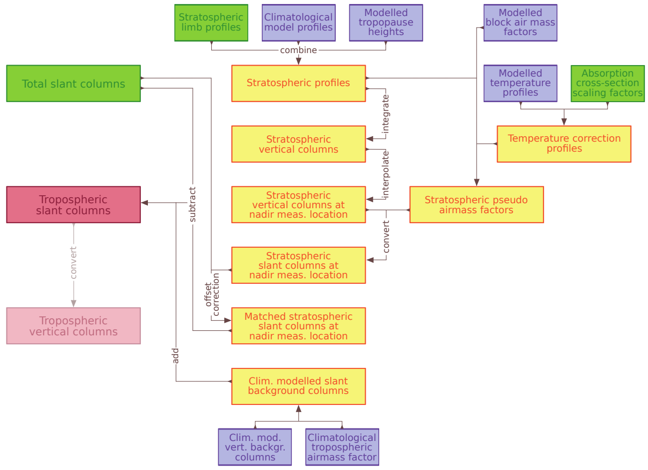

Fig. 1. Data flow of calculating tropospheric NO_2 columns from SCIAMACHY measurements. Measured and modelled quantities are shown in green and purple, respectively, while intermediate results are marked in yellow. Conversion of SCD_{trop} to VCD_{trop} involves calculation of tropospheric air mass factors, the discussion of which is beyond the scope of this study.

to relatively low global coverage, making the derivation of global fields from these measurements a challenging task.

In this study, we calculate one stratospheric NO_2 column for every single SCIAMACHY nadir measurement. Whilst having the disadvantage of not attaining global coverage with the resulting stratospheric data product, this has the advantage of avoiding the need to average over several days of measurements, as, for example, in Beirle et al. (2010). The interpolated VCD_{strat} are then converted to slant columns using stratospheric air mass factors (Sect. 3.3). Following this step, the limb stratospheric slant columns are adjusted to the level of the SCD_{tot} from nadir measurements using an additive offset (Sect. 3.4), taking into account the tropospheric contribution to the measured signal (Sect. 3.5). The full procedure is depicted in Fig. 1.

3.1 Calculating stratospheric NO_2 columns

Based on the measured and modelled number concentration profiles $n^{\mathrm{limb}}(t,h,\varphi,\psi)$ [molec cm^{-3}] and $n^{\mathrm{mod}}(t,h,\varphi,\psi)$ [molec cm^{-3}], respectively, and on the tropopause heights $h_{\mathrm{trop}}(t,\varphi,\psi)$ [m], stratospheric NO_2 profiles are calculated for time t, latitude φ, and longitude ψ as follows: The modelled NO_2 profiles are compiled into a monthly climatology $\overline{n^{\mathrm{mod}}}(m(t),h,\varphi,\psi)$. Let $h^{\mathrm{limb}}_{\mathrm{min}}(t,\varphi,\psi)$ the minimum altitude above surface for which a reliable number concentration has been retrieved from the limb radiances. We define the combined stratospheric profile as

$$n_{\text{strat}}^{\text{limb}}(t,h,\varphi,\psi) = \begin{cases} 0 & \text{if } h < h_{\text{trop}}(t,\varphi,\psi) \\ \overline{n^{\text{mod}}}(m(t),h,\varphi,\psi) & \text{if } h_{\text{trop}}(t,\varphi,\psi) \le h < h_{\text{min}}^{\text{limb}}(t,\varphi,\psi) \\ n^{\text{limb}}(t,h,\varphi,\psi) & \text{if } h \ge h_{\text{min}}^{\text{limb}}(t,\varphi,\psi). \end{cases} \quad (1)$$

The combined limb/model number density profiles are then vertically integrated into stratospheric columns:

$$\mathrm{VCD}_{\text{strat}}^{\text{limb}}(t,\varphi,\psi) = \int_{h=h_{\text{trop}}(t,\varphi,\psi)}^{\text{TOA}} n_{\text{strat}}^{\text{limb}}(t,h,\varphi,\psi)\,\mathrm{d}h. \quad (2)$$

For the Oslo CTM2, vertical stratospheric columns $\mathrm{VCD}_{\text{strat}}^{\text{mod}}(t,\varphi,\psi)$ are calculated accordingly.

3.2 Interpolation to nadir measurement location

Both the model and the limb stratospheric NO_2 column products used in this study are only available on a horizontal resolution that is much coarser than the spatial extents of individual SCIAMACHY nadir measurements (usually $60 \times 30\,\text{km}^2$). Therefore, we need to interpolate the coarse stratospheric columns to the locations of each SCIAMACHY nadir measurement to ensure the best possible spatial matching.

For SCIAMACHY limb measurements, several steps are required in order to calculate stratospheric NO_2 columns for each nadir measurement, processing each orbit separately. This procedure is illustrated in Fig. 2. First, we assign a fixed azimuth angle to each of the four discrete limb line-of-sight directions, namely $-25°$, $-8°$, $10°$ and $27°$. These angles are chosen to be the mean viewing azimuth angles of those nadir pixels which fall into the field of view of the respective limb state.[1]

Next, we consider the stratospheric NO_2 column density along each line-of-sight as depending only on latitude. For each nadir pixel at time t, latitude φ, and longitude ψ, we calculate four stratospheric columns $\mathrm{VCD}_{\text{strat}}^{\text{i}}(t,\varphi,\psi)$ by linearly interpolating along-track, that is along each viewing direction i. For both limb and nadir measurements, we only take into account the descending parts of the orbit to avoid complications from measurements taken at different local times and therefore photochemical states. Finally, for all nadir pixels, we consider the stratospheric NO_2 column to be a function of the line-of-sight, and linearly interpolate the correct column density from the four column densities previously calculated.

In the case of Oslo CTM2 simulations, the modelled NO_2 columns are interpolated to the location and time of the individual nadir measurements using smoothing cubic splines and linear interpolation, respectively.

[1]In this case a negative angle describes a point west of the nadir point, while a positive angle describes a location east of the nadir point.

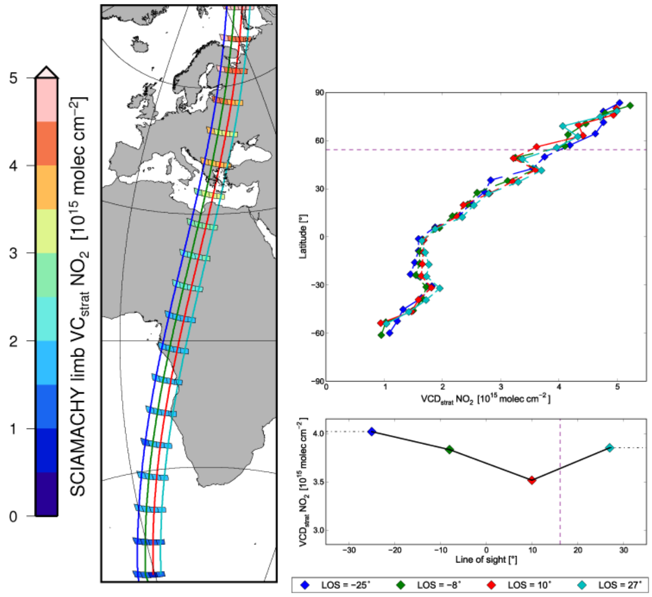

Fig. 2. Interpolation of stratospheric NO_2 columns from SCIAMACHY limb measurements to the location of the same orbit's nadir measurements. As an example, we calculate $\mathrm{VCD}_{\text{strat}}$ for the nadir measurement located at 54.25° N/32.25° E from SCIAMACHY orbit no. 32984 (21 June 2008). In a first step, each limb state is treated independently. For each state, $\mathrm{VCD}_{\text{strat}}$ is considered to be a function of latitude only (left). To calculate a $\mathrm{VCD}_{\text{strat}}$ value for one single nadir measurement, at first, one $\mathrm{VCD}_{\text{strat}}$ per state is calculated by linear interpolation in latitude (top right). Finally, the $\mathrm{VCD}_{\text{strat}}$ value corresponding to the nadir measurement of interest is calculated by linear interpolation in the line-of-sight angle (bottom right).

For ease of notation, we will call the interpolated NO_2 columns again $\mathrm{VCD}_{\text{strat}}^{\text{limb}}(t,\varphi,\psi)$ and $\mathrm{VCD}_{\text{strat}}^{\text{mod}}(t,\varphi,\psi)$ for SCIAMACHY limb and Oslo CTM2, respectively.

Monthly averages of $\mathrm{VCD}_{\text{strat}}^{\text{limb}}(t,\varphi,\psi)$, gridded to 0.125°, are shown in Fig. 3.

3.3 Stratospheric air mass factor (AMF)

We use the radiative transfer model SCIATRAN (Rozanov et al., 2005b) to calculate a lookup table of block air mass factors (BAMF) for 31 solar zenith angles ϑ (SZA) between 10° and 92°, and for 101 uniformly spaced altitude layers h from sea level (0 km) to 100 km.

The NO_2 absorption cross section has a well-known dependence on temperature (Burrows et al., 1998). Boersma et al. (2004) have suggested a simple linear approach to correct for this effect in the retrieval of tropospheric NO_2 columns. The NO_2 absorption cross section used in the DOAS fit was measured at a fixed temperature of 243 K. At very low stratospheric temperatures, the cross section representing the actual atmospheric conditions is therefore larger than the one used in the retrieval, leading to an

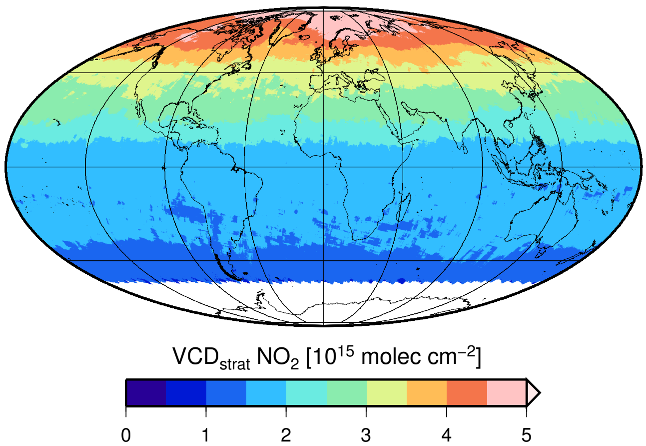

Fig. 3. Monthly averages of VCD_{strat}^{limb} NO_2 from SCIAMACHY limb measurements for June 2010, interpolated to the locations of the SCIAMACHY nadir measurements, and binned to 0.125°.

overestimation of the stratospheric NO_2 column. This will subsequently be corrected for by an increased air mass factor.[2] To these means, we introduce the correction function $f_{tcorr}(T)$, based on the idea presented in Boersma et al. (2004):

$$f_{tcorr}(T) = \frac{3.826 \times 10^{-3} \times T + 0.1372}{3.826 \times 10^{-3} \times T_0 + 0.1372}. \tag{3}$$

This correction function has been derived by comparing differential cross sections measured at four distinct temperatures between 221 K and 293 K and is described by Nüß et al. (2006). T_0 is the temperature at which the cross section used in the fit has been measured; in our case, $T_0 = 243\,K$. The stratospheric air mass factor at time t, latitude φ, longitude ψ, SZA ϑ and viewing zenith angle α is then calculated as

$$AMF_{strat}^{limb} = \left(\frac{1}{\cos\alpha} - 1\right) + \int_{h=h_{trop}}^{TOA} \frac{BAMF \times n_{strat}^{limb}}{f_{tcorr}(T) \times VCD_{strat}^{limb}}\, dh, \tag{4}$$

and accordingly AMF_{strat}^{mod} for Oslo CTM2.

Temporal and spatial interpolation is done as described in Sect. 3.2, while the SZA interpolation is linear.

3.4 Offset limb/nadir

The stratospheric vertical columns derived from SCIAMACHY limb measurements and Oslo CTM2 simulations differ considerably from total vertical columns obtained over the clean Pacific region from SCIAMACHY nadir measurements by applying a stratospheric air mass factor, which we call VCD_{strat}^{nadir}[3]. In this study, we will use the Pacific region

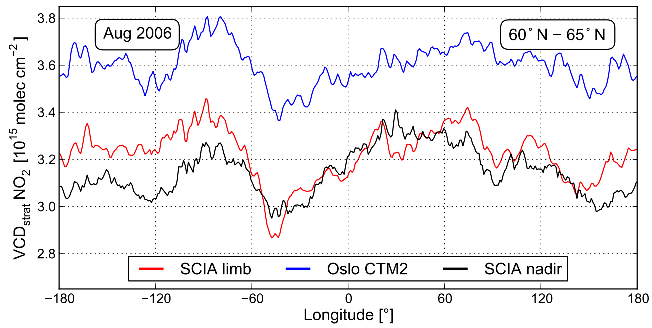

Fig. 4. Zonal variation of VCD_{strat}^{limb} from SCIAMACHY limb measurements (red), VCD_{strat}^{mod} from Oslo CTM2 simulations (blue), and of VCD_{strat}^{nadir} from SCIAMACHY nadir measurements. Monthly mean values for August 2006, between 60° and 65° N.

between longitudes 180° W and 150° W to correct for this effect. This region will subsequently be called "reference sector". An example of the latitude- and time-dependent offset is shown in Fig. 4 for northern latitudes in August 2006.

In order to account for these systematic biases, we apply a daily, latitude-dependent offset to all limb and modelled stratospheric columns to force them to the base level of the nadir measurements.

3.5 Pacific background

Before the stratospheric columns from SCIAMACHY and Oslo CTM2 can be adjusted to the level of the total nadir columns over the Pacific, the latter must be corrected for possible tropospheric NO_2 signals. As independent, appropriate measurements over the Pacific Ocean are extremely sparse, we use climatological NO_2 data derived from the same run of the Oslo CTM2 model as used for the stratospheric columns (see Sect. 2.4). The data show that the tropospheric NO_2 content over the Pacific Ocean is negligibly small most of the time. Only in northern mid-latitudes, and there especially during winter, significant amounts of tropospheric NO_2 are predicted by the model (see Fig. 5).

These enhanced NO_2 columns can most probably be attributed to exported pollution from Eastern Asia and North America, as the lifetime of tropospheric NO_2 is strongly enhanced during winter.

Similar corrections have been previously performed by Martin et al. (2002).

From the modelled NO_2 fields $n^{mod}(t, h, \varphi, \psi)$ [molec cm^{-3}], we calculate vertical tropospheric columns over the reference sector as

$$VCD_{trop}^{mod}(t, \varphi, \psi) = \int_{h=0}^{h_{trop}(t,\varphi,\psi)} n^{mod}(t, h, \varphi, \psi)\, dh. \tag{5}$$

These columns are then compiled into a monthly climatology $VCR_{trop}^{mod}(m, \varphi)$ over the reference sector.

[2] To be precise, one should speak of pseudo air mass factors when they incorporate the temperature correction.

[3] VCD_{strat}^{nadir} still contains the tropospheric contribution to the measured signal.

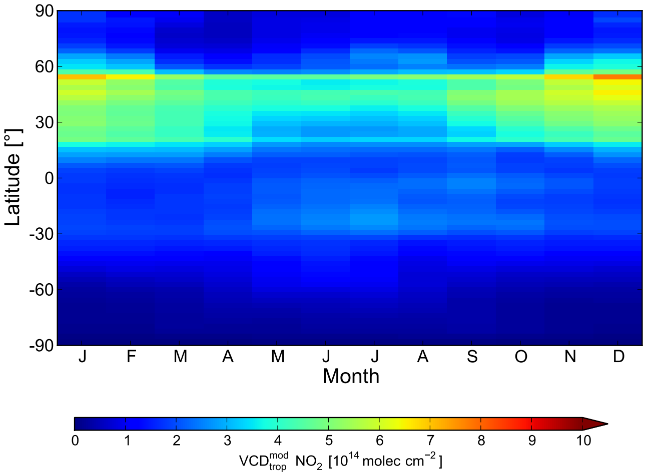

Fig. 5. Climatology of $\mathrm{VCR}_{\mathrm{trop}}^{\mathrm{mod}}$ NO_2 over the Pacific Ocean (180° W–150° W) for the years 1998–2007, computed from Oslo CTM2 simulations.

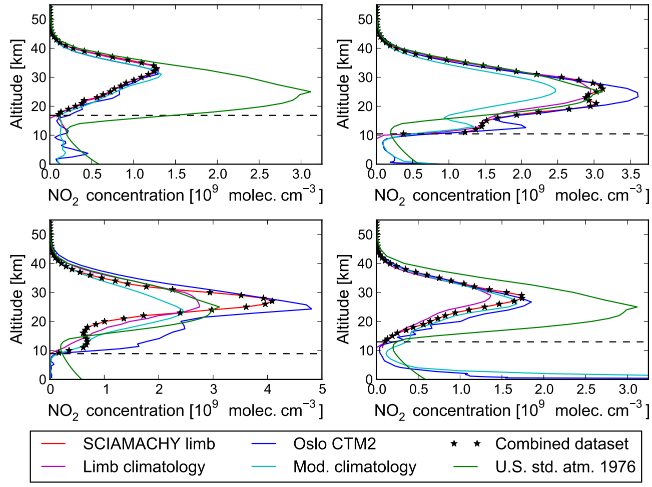

Fig. 6. Vertical NO_2 profiles from SCIAMACHY limb (actual measurement: red, climatology: magenta), Oslo CTM2 (actual value: blue, climatology: cyan), and US Standard Atmosphere 1976 (green) for 1 June 2007, at 3.48° W, 58.66° N (top left); 2 July 2007, at 58.54° W, 63.7° N (top right); 18 February 2007, at 70.54° W, 75.50° S (bottom left); and 27 March 2006, at 5.17° E, 40.65° N (bottom right). The tropopause altitude is shown as a black dashed line, while the combined limb measurements/model climatology profile used for the column and air mass factor calculations in this study are marked as black stars.

As tropospheric air mass factors, we use the dataset developed by Nüß (2005), which was derived using the radiative transfer model SCIATRAN (Rozanov et al., 2005b) and NO_2 profiles from the MOZART4 model. We compile a monthly climatology of air mass factors over the reference sector $\mathrm{AMFR}_{\mathrm{trop}}(m,\varphi)$ by zonally averaging over the $\mathrm{AMF}_{\mathrm{trop}}$ for all SCIAMACHY nadir measurements in month m and at latitude φ over the reference sector during the 2003–2011 time period.

The monthly climatology of modelled tropospheric background columns is then converted to slant columns via

$$\mathrm{SCR}_{\mathrm{trop}}^{\mathrm{mod}}(m,\varphi)=\mathrm{VCR}_{\mathrm{trop}}^{\mathrm{mod}}(m,\varphi)\times\mathrm{AMFR}_{\mathrm{trop}}(m,\varphi). \quad (6)$$

3.6 Applying stratospheric correction

We calculate the stratospheric slant columns on a daily basis. The limb, nadir, and modelled datasets are compiled into zonally averaged daily aggregates over the reference sector, yielding $\mathrm{SCR}_{\mathrm{strat}}^{\mathrm{limb}}(t,\varphi)$, $\mathrm{SCR}_{\mathrm{strat}}^{\mathrm{nadir}}(t,\varphi)$, and $\mathrm{SCR}_{\mathrm{strat}}^{\mathrm{mod}}(t,\varphi)$, respectively. These daily averages are then linearly interpolated in latitude, and smoothed temporally, to account for days and latitudes with missing measurements over the Pacific Ocean. We call the resulting quantities $\mathrm{SCR}_{\mathrm{strat}}^{\mathrm{limb}}(d,\varphi)$, $\mathrm{SCR}_{\mathrm{strat}}^{\mathrm{nadir}}(d,\varphi)$, and $\mathrm{SCR}_{\mathrm{strat}}^{\mathrm{mod}}(d,\varphi)$.

The desired stratospheric slant columns are then calculated by applying the additive offset, derived from the averaged limb (or model) and nadir columns over the reference sector, and forcing the resulting tropospheric slant columns to equal the modelled background columns $\mathrm{SCR}_{\mathrm{trop}}^{\mathrm{mod}}(m,\varphi)$:

$$\begin{aligned}\mathrm{SCD}_{\mathrm{strat}}^{\mathrm{limb}} = \mathrm{VCD}_{\mathrm{strat}}^{\mathrm{limb}}\times\mathrm{AMF}_{\mathrm{strat}}^{\mathrm{limb}}+\\ \mathrm{SCR}_{\mathrm{tot}}^{\mathrm{nadir}}-\mathrm{SCR}_{\mathrm{strat}}^{\mathrm{limb}}-\mathrm{SCR}_{\mathrm{trop}}^{\mathrm{mod}}\end{aligned} \quad (7)$$

and accordingly $\mathrm{SCD}_{\mathrm{strat}}^{\mathrm{mod}}$ for Oslo CTM2.

These $\mathrm{SCD}_{\mathrm{strat}}^{\mathrm{limb/mod}}(t,\varphi,\psi)$ are the final output of our stratospheric correction algorithm. They can be directly subtracted from retrieved nadir total slant columns to yield tropospheric slant columns.

4 Results and discussion

4.1 Stratospheric NO_2 from SCIAMACHY limb and Oslo CTM2

4.1.1 Vertical profiles

As described in Sect. 3.1, we extend the SCIAMACHY limb profiles down to the tropopause, using climatological profiles from the Oslo CTM2 simulations for the years 1998–2007. Figure 6 illustrates that this approach is valid: the profiles measured by SCIAMACHY are similar enough to the climatology of those modelled by Oslo CTM2, especially in the altitude regions between the tropopause and 11 km, where NO_2 concentrations are relatively small.

In some cases, however, the modelled profiles show additional details in the 10–15 km altitude range, which are not detected by the SCIAMACHY sensor. The top right profile in Fig. 6, for example, shows a layer of increased NO_2 concentrations around 14 km altitude. This is not a random fluctuation, as the feature is also seen in the climatological model profiles; on the other hand, such sharp peaks are not visible

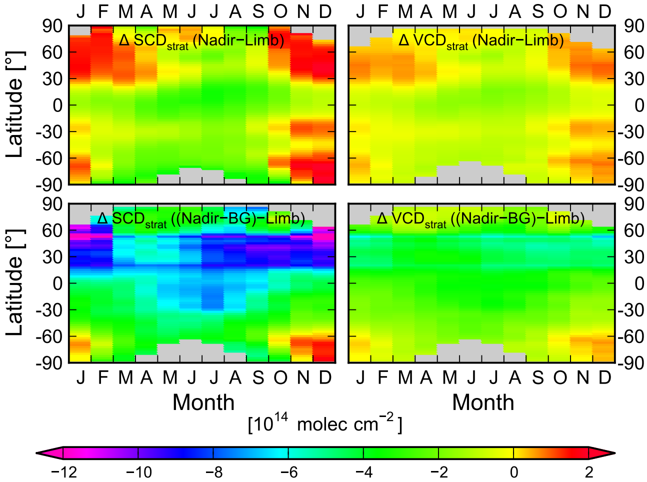

Fig. 7. Monthly climatology of the difference between SCIAMACHY nadir and limb measurements over the Pacific Ocean (180° W–150° W), averaged from the years 2004–2010 and gridded into 2.5° latitude bins. ΔVCD_{strat} (left) and ΔSCD_{strat} (right), "raw" columns (top) and after subtracting the tropospheric influence from the Oslo CTM2 climatology (bottom).

to the SCIAMACHY instrument due to vertical smoothing. At that time of year (early July) and in those latitude regions (65° N), the ECMWF-IFS temperature fields show a layer of enhanced temperature around 14 km. This could drive the decomposition of N_2O_5 and HO_2NO_2, two species which are especially sensitive to temperature changes, leading to increased NO_2 concentrations. Since this feature can be observed at all longitudes, the increased temperature and NO_2 are unlikely to be caused by terrain effects. In these situations, the stratospheric columns resulting from SCIAMACHY observations will be a few percent smaller than those from the model.

4.1.2 Difference to nadir measurements

As described in Sect. 3.4, the NO_2 columns retrieved from SCIAMACHY nadir and limb measurements show a systematic offset. This offset has already been observed previously (Beirle et al., 2010). Figure 7 (top) shows the magnitude of this offset over the Pacific Ocean (180° W–150° W). It ranges from $+3 \times 10^{14}$ molec cm^{-2} in near-polar latitudes in December to -4×10^{14} molec cm^{-2} in polar latitudes in austral winter. In the tropics and mid-latitudes, the offset varies between -1×10^{14} and -3×10^{14} molec cm^{-2}, with a minimum in June/July. The same annual cycle can be observed in all latitude bands, with minima in June and July, and maxima in December and January. In the months October to March, outside the tropics, nadir columns can be larger than limb columns by about 5–6 $\times 10^{14}$ molec cm^{-2} in individual months.

However, the measured nadir columns still contain a tropospheric contribution. After subtracting this modelled background signal (see Sect. 3.5), the stratospheric NO_2 from limb measurements is higher than from nadir geometry almost globally. Only in austral summer, nadir measurements show larger NO_2 values than limb (Fig. 7, bottom). This could point to possible issues in the nadir retrieval from SCIAMACHY measurements, as Richter et al. (2011) reported that over clean background regions, vertical NO_2 columns from SCIAMACHY are smaller than those from GOME-2 by 2–3 $\times 10^{14}$ molec cm^{-2} – too much to be solely explained by diurnal differences caused by the local measurement time. Another possible explanation might lie in the different wavelength windows used for the retrievals (425–450 nm vs. 420–470 nm for nadir and limb, respectively); however, this seems unlikely to be the only cause.

The offset shows both a clear seasonal cycle and strong meridional variation. The seasonal variation suggests that in regions where frontal systems are modulating the tropopause height, we might be observing a varying systematic difference between limb and nadir measurements. The latitudinal variability of the offset looks very similar to that of the modelled background climatology, suggesting that the Oslo CTM2 overestimates the lifetime of tropospheric NO_2, especially in winter.

While generally the observed differences are small in absolute numbers and are well within the expected uncertainties of the two measurements, they do have a significant effect on the retrieved tropospheric columns and therefore need to be corrected for. Overall, further work is needed to investigate this phenomenon in more detail. In the study of tropospheric NO_2, which is dominated by lower atmospheric sources and chemical removal of NO_x, the taken approach for empirically removing its effect is however appropriate.

4.1.3 Climatological comparison measurement/model

To compare measured and modelled stratospheric NO_2 columns, we calculate their correlation for the five years 2003–2007 for which both measurements and model results are available. Figure 8 shows a scatter plot of the monthly mean values of the VCD_{strat} NO_2 between 60° S and 60° N, interpolated to the locations (and, for the model data, times) of the nadir measurements, and gridded to a 0.125° grid. The Pearson correlation coefficient of the two gridded datasets is 0.974, showing excellent correlation. However, the Oslo CTM2 consistently overestimates the measured NO_2 columns, which can be seen from the slope of 0.94. When all latitudes are considered, the correlation coefficient almost remains unchanged, while the slope of the correlation line decreases to 0.88, showing systematically larger stratospheric NO_2 columns from the model at high latitudes. From the comparison of the measured and modelled vertical profiles, it becomes apparent that the systematic overestimation is mostly coming from altitudes lower than 30 km (see Sect. 4.1.1).

The spatial patterns in VCD_{strat} NO_2 from SCIAMACHY limb measurements and Oslo CTM2 simulations agree

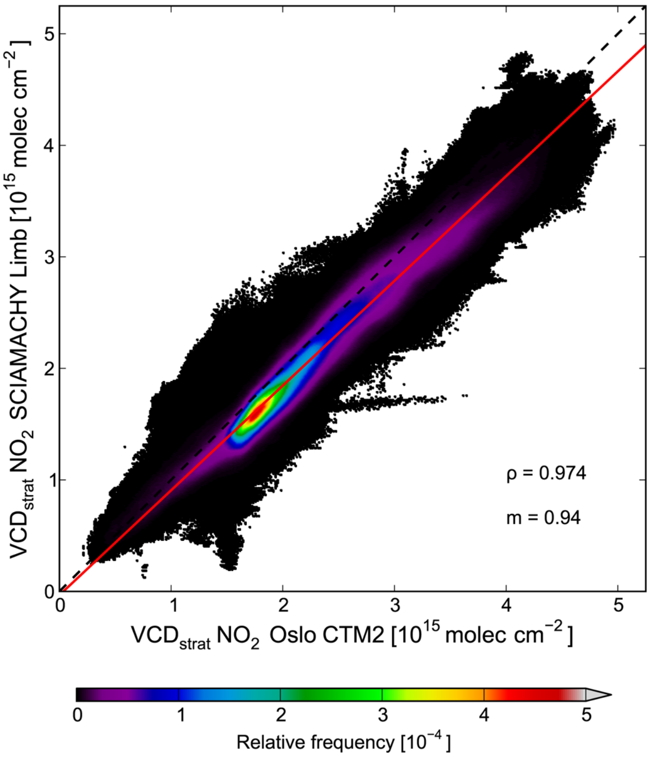

Fig. 8. Scatter plot of monthly mean values for VCD_{strat} NO_2 from SCIAMACHY limb measurements and Oslo CTM2 simulations for the 2003–2007 time period, for the latitudes between 60° S and 60° N. The red line marks the linear regression fit (slope 0.94, offset -3.3×10^{13}). The Pearson correlation coefficient of the two datasets is 0.974.

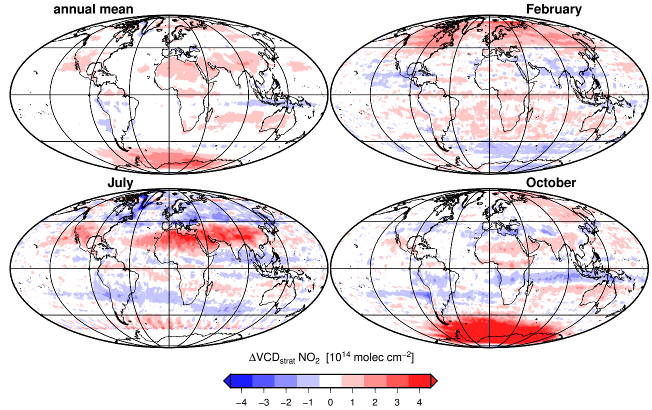

Fig. 9. The difference ΔVCD_{strat} NO_2 between SCIAMACHY limb and Oslo CTM2 for the 2003–2007 time period. Red and blue areas correspond to regions where SCIAMACHY limb measurements are larger and smaller than Oslo CTM2 simulations, respectively. Top left: average difference over all months. Top right: average difference of all Februaries. Bottom left: average difference of all Julies. Bottom right: average difference of all Octobers. An additive offset has been applied to force the difference to equal zero over the reference sector (180° W–150° W).

remarkably well, after removing an offset between the two datasets. Figure 9 shows the average difference between the two datasets for the 2003–2007 period and for three selected climatological monthly means.[4] The difference of the five-year averages has been offset so that it amounts to 0 over the reference sector (180° W–150° W). Systematic differences in the vertical columns are smaller than 5×10^{13} molec cm^{-2}. The spatial pattern of these differences is interesting, showing a clear seasonality and, in some regions, e.g. the South American west coast, a strong land–sea contrast. One possible explanation might be an orographic effect stemming from the comparably low resolution of the Oslo CTM2. Another possible source for the observed spatial patterns might be the model's treatment of clouds and their influence on photochemistry; however, the photochemistry is mostly determined by the short wavelengths, which usually do not penetrate deep enough to be affected by clouds, especially at high latitudes.

The possible influence of clouds has been investigated by filtering for scenes with less than 20 % cloud cover from the FRESCO+ dataset (version 6, Wang et al., 2008). In general, our findings show that clouds cannot be made responsible for the observed spatial patterns. The only exceptions are the Antarctic coast, where the cloud-screened data lack the large area of positive differences seen in the full dataset, and the Canadian Hudson Bay area, where the difference in the cloud-screened data turns negative from the positive values in the full dataset. In the case of the Antarctic coast, the large positive differences come mostly from austral spring (September and October). Both effects can, most probably, be attributed to the FRESCO+ cloud algorithm having difficulties in identifying clouds over bright surfaces, which in turn leads to an under-representation of winter values in the climatological average.

The impact of clouds should be explored further, because the understanding of the systematic differences between limb retrievals and model simulations might improve our knowledge of the influence of clouds and surface spectral reflectance on atmospheric photochemistry.

4.1.4 Zonal variability of stratospheric NO_2 columns

A detailed comparison between the two offset-corrected stratospheric datasets has been carried out on the level of monthly averages. Gridded data points have been binned into boxes of 1° longitude × 5° latitude. Here, we compare the results of the correction algorithm which we presented in Sect. 3, namely stratospheric vertical columns NO_2, derived

[4] See Supplement for plots of the months not shown in Fig. 9.

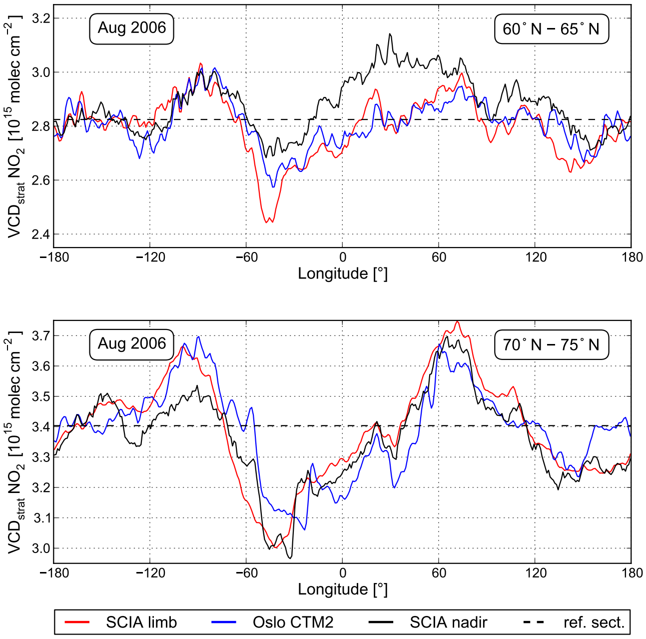

Fig. 10. Zonal variation of VCD'^{limb}_{strat}, VCD'^{mod}_{strat}, and VCD'^{nadir}_{strat}. The nadir measurements' value over the reference sector is marked as dashed black line. Monthly mean values for August 2006, between 60° and 65° N (top) and between 70° and 75° N (bottom).

from the offset-corrected SCD^{limb}_{strat} and SCD^{mod}_{strat} via

$$VCD'^{limb}_{strat} = \frac{SCD^{limb}_{strat}}{AMF^{limb}_{strat}} \tag{8}$$

$$VCD'^{mod}_{strat} = \frac{SCD^{mod}_{strat}}{AMF^{mod}_{strat}}. \tag{9}$$

For comparison, we show the "stratospheric" vertical column derived from SCIAMACHY nadir measurements as

$$VCD'^{nadir}_{strat} = \frac{SCD^{nadir}_{tot} - SCR^{mod}_{trop}}{AMF^{limb}_{strat}}. \tag{10}$$

First, it is noticeable that the zonal variability of SCIAMACHY limb measurements and Oslo CTM2 simulations is remarkably similar (see Fig. 10, top). However, the simulated stratospheric columns are often larger than the measured values, which is also shown by the linear regression of the two datasets (cf. Fig. 8). The two stratospheric datasets agree reasonably well with the nadir measurements in unpolluted regions (see Fig. 10, top).

One noticeable feature in all datasets is a systematic low in the observed VCD_{strat} NO_2 over Greenland ($\sim$ 50° W) in summer (June–September), a pattern which can be seen in all years 2003–2011 (see Fig. 10 for August 2006). Since this feature is present in both datasets and persistent over the years, we deem it unlikely to be a retrieval or modelling artifact. The area of southern Greenland is known to be special for multiple reasons. There exists strong tropopause

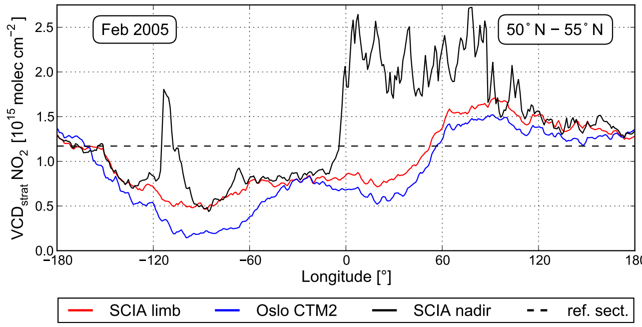

Fig. 11. Zonal variation of VCD'^{limb}_{strat}, VCD'^{mod}_{strat}, and VCD'^{nadir}_{strat}. The nadir measurements' value over the reference sector is marked as dashed black line. Monthly mean values for February 2005, between 50° and 55° N.

folding activity (Elbern et al., 1998) and thus troposphere-stratosphere exchange (Sprenger and Wernli, 2003). Furthermore, a local maximum in the density of polar low pressure systems exists to its east (see Zahn and von Storch, 2008), and Greenland's high surface altitude and high surface reflectance (due to ice cover) stand in clear contrast to the surrounding Atlantic Ocean. While all these factors might contribute to the observed summer lows in VCD_{strat} NO_2, the underlying mechanisms remain unclear at the moment, and it is difficult to clearly attribute this phenomenon to one of them.

While generally the shape of the zonal variation is very similar between SCIAMACHY limb and Oslo CTM2, in some cases, the amplitudes can differ significantly. An example is shown in Fig. 11, where, after applying the offset, the agreement between nadir and limb measurements is mostly excellent in those regions without tropospheric pollution. The simulated VCD'^{mod}_{strat}, however, are slightly lower than the measured ones, indicating that the model might be overestimating the stratospheric NO_2 over the Pacific Ocean, leading to an exaggerated bias correction.

Often, the maxima of stratospheric NO_2 abundances are located over the Pacific Ocean. Reasons for this can be found in the unique geographical conditions: in northern latitudes, it is located over the open ocean and surrounded by the Rocky Mountains in North America and the mountain ranges in East Siberia. This pronounced land–sea contrast strongly influences tropospheric circulation, which in turn might drive stratospheric conditions. The source of the systematic difference between limb and nadir columns might thus be related to NO_2 in the upper troposphere/lower stratosphere (UT/LS) and the tropopause height being modulated by Lee waves, which are generated by the wind system and the topography. It seems that the ECMWF-IFS model (which drives the meteorology in Oslo CTM2) sometimes fails to correctly capture the actual extent of these effects, leading to a slightly overestimated stratospheric NO_2 column over the Pacific Ocean, which in turn would lead to an overestimated tropospheric

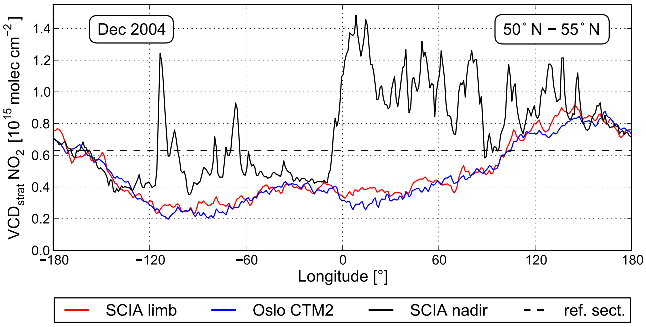

Fig. 12. Zonal variation of VCD'^{limb}_{strat}, VCD'^{mod}_{strat}, and VCD'^{nadir}_{strat}. The nadir measurements' value over the reference sector is marked as dashed black line. Monthly mean values for December 2004, between 50° and 55° N.

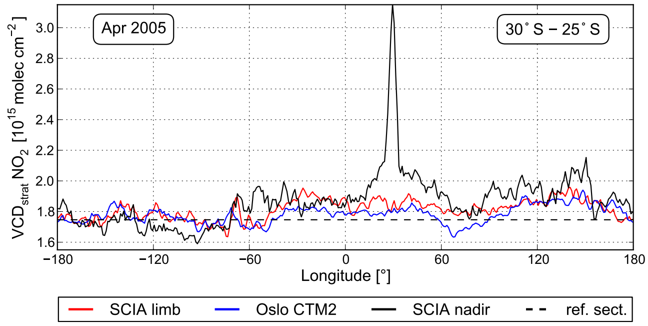

Fig. 13. Zonal variation of VCD'^{limb}_{strat}, VCD'^{mod}_{strat}, and VCD'^{nadir}_{strat}. The nadir measurements' value over the reference sector is marked as dashed black line. Monthly mean values for April 2005, between 30° and 25° S.

NO_2 burden over North America when using the modelled NO_2 fields for stratospheric correction.

In cases like this, the assessment of tropospheric pollution can be severely influenced by the used stratospheric correction, especially over North America. Figure 12 shows another example (January 2005, 50°–55° N), when using the reference sector method, only the pollution signals of the cities Montréal, Toronto and Edmonton would be visible as positive tropospheric columns, but the actual VCD_{trop} would be underestimated by more than 50 %. This is again caused by the fact that the Pacific Ocean stratosphere often contains larger NO_2 columns than the zonally adjacent areas.

Finally, an interesting issue regarding the nadir measurements can be identified by comparing them to limb measurements. In many months, the retrieved nadir columns seem to be lower than the integrated limb stratospheric measurements off the Chilean coast in the East Pacific (∼ 75–80° W). As it can be seen in Fig. 13, the VCD'^{nadir}_{strat} from nadir measurements are lower than those from limb measurements and model simulations by about 1×10^{14} molec cm^{-2}. In this case, it seems not to be an artefact originating from the reference sector offset, as the nadir measurements are significantly higher than the limb measurements at many other longitudes. This might be a hint leading to issues in the nadir retrieval over clean ocean waters, for example from liquid water absorption or vibrational Raman scattering in water (Vountas et al., 2003; Lerot et al., 2010). A more systematic investigation of this is needed, but outside the scope of this study.

4.1.5 Comparison of the day-to-day variability

Particular attention needs to be paid to the variability of the different stratospheric datasets. The very sparse spatial coverage of the limb measurements could lead to large variability of the interpolated data product. As this would severely interfere with its usability for stratospheric correction, we investigate this issue by comparing the variability of the stratospheric vertical columns. For 2005, we calculated daily averages of all data points (measurement pixel centres/model grid cell centres) within 5.6° × 5.6° boxes, located at 180° longitude and nine different latitudes. Figure 14 shows the daily time series. Both limb measurements and modelled columns are taken from the "raw" datasets, i.e. neither spatial interpolation nor offset correction have been applied. Oslo CTM2 values in high latitude winter are unrepresentative since at SCIAMACHY measurement time (to which the modelled data have been interpolated), the sun is still below the horizon, and the model state therefore represents nighttime chemistry.

SCIAMACHY limb measurements generally yield higher VCD_{strat} NO_2 than Oslo CTM2 simulations and SCIAMACHY nadir measurements, at low and mid-latitudes. At very low solar zenith angles, however, Oslo CTM2 simulations show considerably higher NO_2 values, especially in the Southern Hemisphere. This is most probably due to the difficult determination of the average overpass time of one model grid cell at such high latitudes, which might cause significant errors when the overpass time can vary considerably within one model grid cell.

As a measure to compare the variabilities of the three datasets, we compute the coefficients of variation c_V.

We calculate daily residuals by subtracting a centred 31-day moving average from the daily time series (see Fig. 15), and define c_V as the ratio of their standard deviation and sample mean (see Table 1).

In most latitude regions, the variability of limb measurements and modelled columns is quite comparable. In northern mid-latitudes, however, Oslo CTM2 shows a considerably higher variability than SCIAMACHY limb measurements. In all latitude bands, the nadir measurements from SCIAMACHY have a considerably higher c_V than the two other datasets; values for c_V are up to 50 % higher than from limb measurements. The coefficient of variation c_V of the nadir measurements is larger than that of the limb measurements at almost all latitudes, hinting to higher random errors

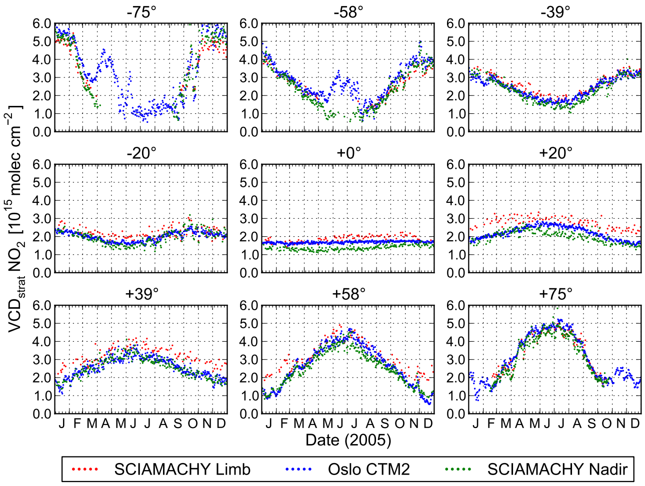

Fig. 14. Daily time series for the year 2005 of $\mathrm{VCD_{strat}}$ NO_2 from SCIAMACHY limb (red), Oslo CTM2 (blue), and of $\mathrm{VCD_{tot}}$ from SCIAMACHY nadir (stratospheric air mass factor applied, green) for nine $5.6° \times 5.6°$ grid boxes. The centres of the grid boxes are located at 180° longitude and the latitudes are given in the plot titles.

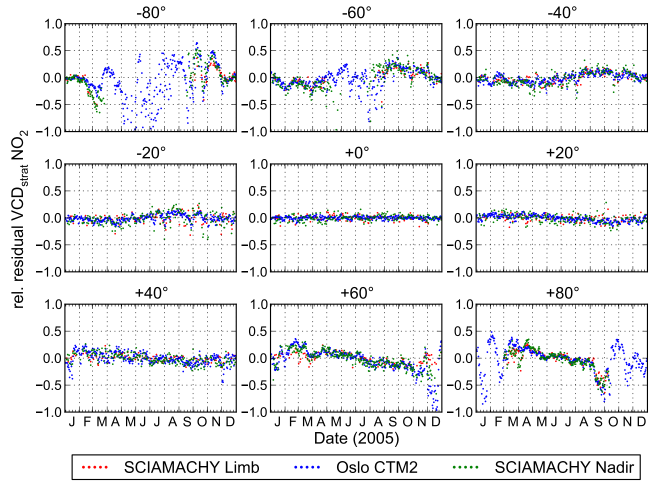

Fig. 15. Time series for the year 2005 of the relative residuals of $\mathrm{VCD_{strat}}$ NO_2 from SCIAMACHY limb (red), Oslo CTM2 (blue), and of $\mathrm{VCD_{tot}}$ from SCIAMACHY nadir (stratospheric air mass factor applied; green) for nine $5.6° \times 5.6°$ grid boxes. The centres of the grid boxes are located at 180° longitude and the latitudes are given in the plot titles. The residuals have been computed by subtracting a centred 31-day moving average from the daily dataset.

in the nadir retrieval as compared to the limb retrieval. We conclude that the measurement noise in the individual limb columns, while being significant, does not severely impact the retrieval of tropospheric NO_2 columns.

4.2 Sensitivity study: impact of air mass factor calculations

As described in Sect. 3.3, the integrated and interpolated $\mathrm{VCD_{strat}}$ need to be converted to slant columns. The simplest approach is to use an air mass factor based on a single atmospheric profile, e.g. the climatological stratospheric NO_2 profile from the US Standard Atmosphere 1976 (Committee on Extension to the Standard Atmosphere, 1976), and to assume a constant surface reflectivity, e.g. 0.05. The influence of the surface reflectivity on the stratospheric AMF is reported to be very low (Wenig et al., 2004), which is why this effect is not further investigated within this study. Figure 16 (bottom left) shows the relative change of the stratospheric AMF introduced by using the actual stratospheric NO_2 profile as measured by SCIAMACHY. In virtually all cases, the influence of the assumed NO_2 profile on the stratospheric air mass factors is negligible. Only in polar latitudes in winter does assuming the stratospheric NO_2 profile from the US Standard Atmosphere lead to an overestimation of stratospheric AMFs by up to 4.5 %.

To assess the influence of the temperature dependence of the NO_2 absorption cross section on the stratospheric NO_2 correction (see Sect. 3.3), we performed a sensitivity study on eight years of data from 2003 until 2010. We used the same ECMWF forecast temperature profiles which were used in the limb retrieval. Our results show that the temperature dependence of the NO_2 absorption cross section actually has significant influence on stratospheric air mass factors. As it can be seen in Fig. 16 (top right), the temperature dependence influences the stratospheric air mass factors by between 5 % and 15 %; using a fixed temperature of 243 K leads to an underestimation of the AMF. The influence is highest for the winter months and can reach up to 15 % at polar latitudes in the climatological mean.

Combined, the two effects cancel out to some degree. When comparing the most accurate $\mathrm{AMF_{strat}}$ (derived using SCIAMACHY profiles and ECMWF temperatures) with the most simple one (using a US Standard Atmosphere profile and disregarding the temperature dependence), our results

Table 1. Coefficients of variation $c_\mathrm{v} = \frac{\sigma}{\mu}$ (σ being the standard deviation, and μ being the sample mean) of daily $\mathrm{VCD_{strat}}$ NO_2 for nine $5.6° \times 5.6°$ grid boxes located at 180° longitude for the year 2005.

Latitude	SCIA limb	SCIA nadir	Oslo CTM2
−80°	0.199	0.359	0.603
−60°	0.328	0.435	0.325
−40°	0.236	0.313	0.233
−20°	0.133	0.205	0.129
0°	0.088	0.091	0.035
20°	0.111	0.156	0.161
40°	0.147	0.226	0.218
60°	0.302	0.370	0.448
80°	0.265	0.298	0.419

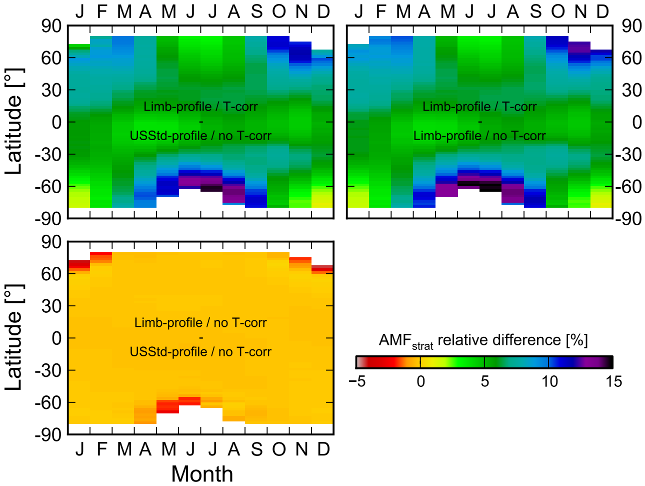

Fig. 16. Monthly climatologies of the influence of stratospheric NO_2 profiles and temperature correction on stratospheric air mass factors. The plots show the influence of both profiles and temperature correction (top left), temperature correction alone (top right), and vertical profiles alone (bottom left). The climatologies are calculated for the years 2003–2010, using all retrieved limb profiles from the descending part of the SCIAMACHY orbit. The influence of the vertical profile is derived by comparing to using the US Standard Atmosphere's NO_2 profile. Stratospheric temperature profiles are taken from the ECMWF forecast (the same profiles used in the limb retrieval). The geometric line-of-sight correction (the summand $\frac{1}{\cos\alpha}-1$) has been ignored in this comparison, and the relative difference of two datasets is computed as $\frac{a-b}{(a+b)/2}$.

show that the simple AMF underestimates the accurate one by ca. 2–14 % (Fig. 16, top left).

4.3 Improvements to the tropospheric data product

When using SCIAMACHY limb measurements or Oslo CTM2 simulations as a stratospheric correction scheme instead of the reference sector method, the data quality of the resulting fields of tropospheric slant columns improves considerably. Figure 17 shows SCD_{trop} NO_2 for February 2005, using the reference sector method, SCIAMACHY limb measurements, and Oslo CTM2 simulations as stratospheric correction schemes. Compared to using the reference sector method, both of the other stratospheric corrections considerably reduce the number of negative tropospheric NO_2 columns.

The SCD_{trop}^{limb} for a single day (28 January 2006) are shown in Fig. 18.[5] Compared to the data shown by Beirle et al. (2010), our results appear to be slightly less noisy. This might be because our approach accounts for possible small-scale variability in stratospheric NO_2 abundances. The most striking difference, however, is the almost complete lack of significantly negative tropospheric NO_2 columns in our data product. This is mostly due to the fact that we account for the NO_2 content of the Pacific troposphere, contrary to the "relative limb correction" of Beirle et al. (2010).

[5]Additional days are shown in the Supplement. All days have been chosen to allow easy comparison to the results of Beirle et al. (2010).

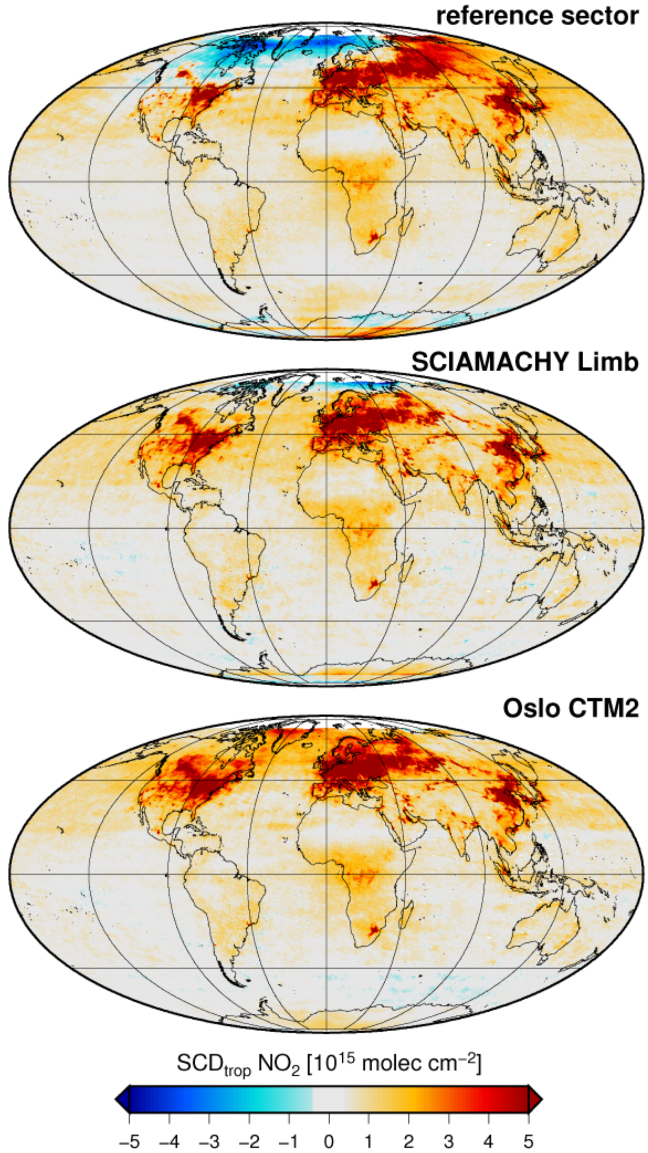

Fig. 17. Monthly average of SCD_{trop} NO_2 from SCIAMACHY for February 2005, using the reference sector method (top), SCIAMACHY limb measurements (centre), and Oslo CTM simulations (bottom) as stratospheric correction.

Another way to evaluate possible improvements to the tropospheric data product is to analyse time series over regions where the reference sector method leads to problematic results. Figure 19 shows time series of SCD_{trop} for the period from October 2002 until May 2011 over four regions with different characteristics. When using the reference sector method for stratospheric correction, the northern

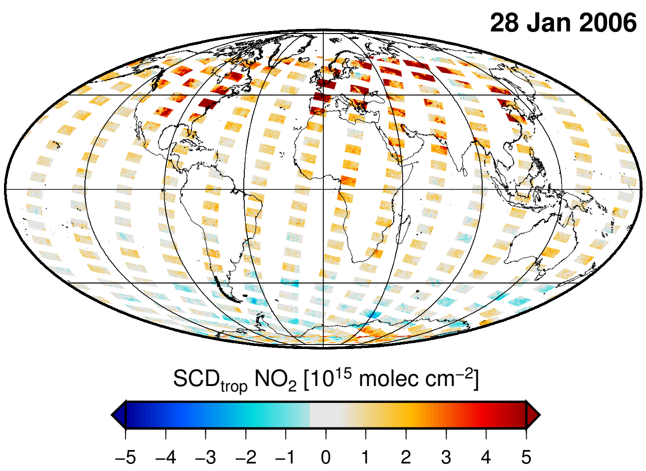

Fig. 18. SCD$_{trop}$ NO_2 from SCIAMACHY for 28 January 2006, using SCIAMACHY limb measurements as stratospheric correction schemes.

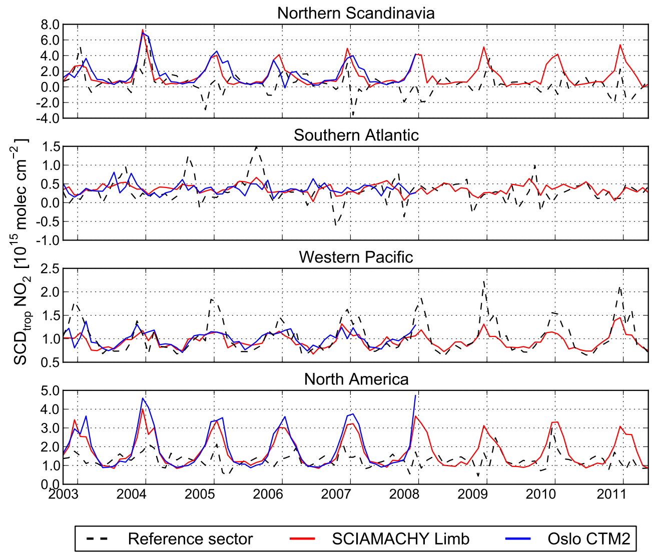

Fig. 19. Time series of monthly mean values of SCD$_{trop}$ NO_2 for the regions labelled above as Northern Scandinavia (60° N–75° N, 0°–40° E), Southern Atlantic (50° S–30° S, 45° W–15° E), Western Pacific (25° N–50° N, 148° E–178° E), and North America (40° N–60° N, 120° W–90 ° W). Three different stratospheric correction schemes have been used: SCIAMACHY limb measurements (red), Oslo CTM2 simulations (blue, only until 2007), and the reference sector method (black).

Scandinavia region shows a very clear seasonal cycle, with large negative values in winter. While the large amplitude of the oscillations is mostly due to the varying measurement geometry, the fact that the monthly mean values are consistently negative results from the observation already made in Sect. 4.1.4, where we showed that, especially in polar winter, stratospheric NO_2 fields are far from being zonally homogeneous. Most often, stratospheric NO_2 between 60° N and 75° N seems to peak over the reference sector – a result which is backed by investigation of the zonal variability of the stratospheric NO_2 products (see Sect. 4.1.4). When using SCIAMACHY limb measurements or Oslo CTM2 simulations for stratospheric correction, these issues appear to be solved. The retrieved slant columns show a clear seasonal cycle with large winter maxima, as is to be expected from measurement geometry and enhanced lifetime of tropospheric NO_2 in winter due to photochemistry. The curves for SCIAMACHY limb and Oslo CTM2 qualitatively agree very well throughout the year, and during summer months, also with the reference sector method.

In the southern Atlantic region, results are similar. The large amplitudes of the reference sector time series in spring are gone when using limb measurements or Oslo CTM2 simulations for stratospheric correction. However, the SCIAMACHY and Oslo CTM2 datasets do not seem to agree as well. This might be due to the fact that the overall magnitude of the tropospheric slant columns is considerably smaller in this region, leading to a higher relative influence of the uncertainty in the stratospheric columns on the time series.

In the western Pacific region, a clear seasonal cycle can be seen independently of the used stratospheric correction. During the summer months, all three datasets agree very well. During winter, however, the tropospheric slant columns retrieved using the reference sector method are considerably larger than the other two datasets, by as much as 60 %. This interesting feature might hint towards higher stratospheric NO_2 columns in this region compared to the reference sector, which is directly neighbouring to the east. While this observation is supported by the plots of zonal variability in Sect. 4.1.4, the reason for this repeating pattern is unclear.

Over North America, finally, the reference sector method leads to a clear underestimation of tropospheric pollution levels in winter. When either SCIAMACHY limb measurements or Oslo CTM2 simulations are used for stratospheric correction, however, the seasonal cycle becomes a lot more pronounced. The tropospheric columns in winter more than double in many years, while the summer lows remain almost unchanged.

4.4 Error analysis

4.4.1 Errors in the nadir measurements

Several different sources contribute to the total error in the slant columns measured by SCIAMACHY in nadir geometry. The uncertainties in the measured radiances lead to a random error in the DOAS fitting procedure. Systematic errors can be introduced by the absorption cross sections used in the DOAS fit. Inaccuracies in the fitting procedure, e.g. errors in the estimation of water leaving radiance, lead to retrieval errors. One issue could be identified off the Chilean coast, where nadir measurements are lower than limb measurements by approximately 10^{14} molec cm^{-2}. In total, the retrieval errors amount to approximately 4×10^{14} molec cm^{-2} for the retrieved slant columns, which is less than 5 % (Richter et al., 1998; Boersma et al., 2004; Wenig et al., 2004).

Additionally, the nadir columns are subject to errors introduced by air mass factor calculations. For tropospheric columns over polluted regions, this is the dominating error source, which has been discussed elsewhere (Boersma et al., 2004; Leitão et al., 2010; Heckel et al., 2011). Here, only the uncertainties introduced into the stratospheric contribution of the signal are of interest. The vertical NO_2 profiles (taken from the limb measurements) as well as the temperatures from the ERA-Interim reanalysis both contribute to these errors, but are difficult to quantify. The sensitivities of the resulting air mass factors to changes in the vertical absorber profile and to the temperature profile are given in Fig. 16, showing that uncertainties in these two quantities do not contribute significantly to the total error in most cases.

4.4.2 Errors in the limb measurements

Random errors in the measured radiances and systematic errors due to inaccuracies in the used absorption cross sections can influence the limb retrieval as well as the nadir retrieval. Instrument pointing errors can impact on the vertical resolution and position of the measured profiles, and the retrieval sensitivity decreases at lower altitudes. These error sources are discussed in detail in Bauer et al. (2012) and Rozanov et al. (2005a), and are expected to add up to less than 15 % of the VCD_{strat} in most cases.

In those cases when the tropopause layer lies below the lower boundary of the limb profiles at 11 km, we extend the measured limb profiles with climatological profiles derived from Oslo CTM2 simulations (see Sect. 2.2). Errors in the climatological modelled vertical profiles can thus contribute to the total error of the stratospheric columns. However, our comparison of modelled and measured profiles shows that this effect can generally be neglected, as NO_2 number concentrations in the UT/LS region are very low (see Fig. 6).

One further uncertainty comes from the radiative transfer modelling. Air masses from far away can contribute to the limb signal reaching the satellite, and spatial gradients can further complicate the situation. This effect has been studied in great detail in Pukı̄te et al. (2010). Depending on the tangent height, the errors introduced to the retrieved NO_2 concentrations can be as large as 20 %. Pukı̄te et al. (2010) show that these errors can be avoided by using a tomographic 2-D approach in the radiative transfer calculations. It is however not applicable in an operational data product, as it only improves the profile retrieval in the case of reduced distance between the individual SCIAMACHY measurements (3.3°) obtained in dedicated limb-only orbits. Based on the findings of Pukı̄te et al. (2010), we estimate the upper boundary of the error on the retrieved stratospheric columns to be 30 % in some rare extreme cases of low absolute values, while in most situations, the associated error should not exceed 10 % of the VCD_{strat}.

4.4.3 Errors in the resulting tropospheric slant columns

Uncertainties in the tropospheric slant columns derived by the limb/nadir matching approach are determined by the uncertainties in both the nadir and limb observations as well as the model background added over the Pacific Ocean. Our study suggests that the random error in the stratospheric columns retrieved from limb measurements is of the same magnitude as the one for nadir measurements (see Table 1), leading to an increase of the random errors in the resulting tropospheric slant columns by a factor of approximately $\sqrt{2}$. Assuming a 10 % random uncertainty in the limb columns, and maximum stratospheric slant columns of about 1×10^{16} molec cm^{-2} at latitudes below 60°, errors of up to 1×10^{15} molec cm^{-2} can be introduced. Systematic errors are to a large extent removed by adjusting the limb columns over the reference sector, but longitude-dependent offsets between limb and nadir measurements might still exist. Also, it must be noted that in cases when the visibility of tropospheric NO_2 is reduced by cloud coverage in the reference sector, the offset correction might lead to an underestimation of the stratospheric slant columns and thus yield too high tropospheric columns. The resulting uncertainty in the tropospheric slant columns is bounded by the NO_2 content of the Pacific troposphere and thus on the order of 2–4×10^{14} molec cm^{-2} in most regions and times; only in the Northern Hemisphere winter are considerable amounts of NO_2 predicted by the Oslo CTM2 model, leading to possibly larger errors. However, it must be noted that currently, accepting this uncertainty seems to be unavoidable. While excluding cloudy pixels from the calculation of SCD_{tot}^{nadir} for determining the Pacific offset correction would avoid the systematic underestimation of stratospheric slant columns, the cloud filter would remove a large amount of all measurements over the Pacific, considerably increasing the influence of random errors and noise (which would cancel out to a large extent with a higher number of measurements) on the data product. On the other hand, explicitly accounting for clouds in the calculation of AMF_{trop} is almost impossible, because both NO_2 and clouds are mostly found in the free troposphere and no measurements of their relative vertical distribution exist on a regular and global scale.

While it is difficult to quantify such uncertainties, a careful study of the climatological differences between measured and modelled stratospheric columns can lead towards a better understanding of problematic regions (see Fig. 9). In early boreal spring, the measured vertical columns are significantly higher than the modelled columns in northern high and midlatitudes by approximately 3×10^{14} molec cm^{-2}. In July, on the other hand, the measured columns are lower than the modelled ones over almost all of the Eurasian continent by up to 2×10^{14} molec cm^{-2}. Furthermore, the systematic differences exhibit a stripe structure in the subtropics and mid-latitudes between South America and Australia. Likewise, in July, modelled stratospheric columns are significantly higher than measured ones along the western coast of Greenland. This feature can clearly be attributed to the limb measurements, because the systematic under-estimation of the limb-measured columns is also visible in the climatological difference between SCIAMACHY limb and nadir columns (see Supplement). In October, stratospheric columns modelled by Oslo CTM2 are considerably lower in the southern polar region than SCIAMACHY's limb columns. This is in accordance with Beirle et al. (2010) (Fig. S16 therein), who show that at the same time and region, their SCIAMACHY limb columns are considerably higher than their nadir columns, using their SCD_{trop}. This feature is also present in our data (not shown). It is difficult to clearly attribute these differences to either of the datasets; however, they must be considered in the estimation of the uncertainties. Also in October, a streaky pattern similar to the one observed in July can be seen over the Indian Ocean; the sign of the differences is however reversed, and their magnitude amounts to up to 2×10^{14} molec cm^{-2}.

The impact of these differences on the tropospheric slant columns depends on the corresponding stratospheric air mass factors, which are typically of the order of 2–3 over low and mid-latitudes, but can be as large as 9 at 85° SZA (high latitudes in winter). The systematic differences highlighted above therefore correspond to tropospheric slant column uncertainties of usually up to 5×10^{14} molec cm^{-2}, but can be as large as 2.5×10^{15} molec cm^{-2} at high latitudes in winter.

Over polluted regions, the bulk of tropospheric NO_2 abundances is located in the boundary layer, leading to a one-to-one translation of these systematic errors in the slant columns to errors in the vertical columns because the tropospheric air mass factor is close to one. In these cases, the uncertainties in the vertical columns only contribute a small relative fraction to the large measured quantities. In cleaner regions, the tropospheric air mass factor is larger than one and approaching the stratospheric AMF, leading to smaller absolute contributions of the stratospheric correction scheme to the total errors in the tropospheric vertical columns. We conclude that in most polluted cases, the relative importance of the error introduced by the limb stratospheric correction is rather small, but care must be taken over clean regions and those areas highlighted above, where model and measurements show larger deviations.

5 Summary and conclusions

In the present study, we implemented the direct limb/nadir matching method to correct for the stratospheric contribution to total slant columns of NO_2 retrieved using the DOAS technique from SCIAMACHY nadir measurements. The use of SCIAMACHY limb measurements was compared to the simple reference sector method and to using stratospheric NO_2 columns modelled with the Oslo CTM2. In contrast to previous studies, we interpolate one stratospheric NO_2 value for every single nadir-mode measurement made by SCIAMACHY using only the limb data taken in the same orbit. This leads to a very accurate representation of the zonal variability of stratospheric NO_2, avoiding the problems arising from spatiotemporal averaging. However, this advantage comes at the cost of creating a stratospheric correction method tailor-made for SCIAMACHY nadir measurements – the interpolation scheme described in this study cannot be applied to other satellite sensors like, e.g. GOME-2.

Both SCIAMACHY limb measurements and Oslo CTM2 simulations provide a significant and important improvement compared to the reference sector method. However, neither of the datasets can be applied as an absolute correction. They both need to be corrected for a systematic bias by shifting them to the level of the nadir measurements over a clean region in the Pacific Ocean. After this offset correction, the two datasets are found to agree surprisingly well.

For SCIAMACHY limb measurements, Beirle et al. (2010) also had to apply an offset correction. In the case of the Oslo CTM2 simulations, this offset is in principle a very simplistic assimilation scheme. In contrast to the TM4 assimilation used in the retrievals at KNMI (Boersma et al., 2007), our approach is different in that the "assimilation" is not performed online during the model calculations but rather afterwards. On the other hand, Oslo CTM2 features a full chemistry scheme compared to the simpler mechanisms found in TM4 (Dirksen et al., 2011). While measurements of tropospheric NO_2 over the Pacific Ocean are sparse, tropospheric NO_2 abundances must be accounted for in this bias correction. Results from the Oslo CTM2 show that tropospheric NO_2 columns over the reference sector are generally very low, but can reach significant amounts in northern mid-latitudes in winter. Therefore, we have used a climatology based on data from this model to account for the tropospheric background in the data.

The sensitivity of stratospheric air mass factors to actual atmospheric conditions has been analysed as well as the importance of the temperature dependence of the NO_2 absorption cross section. In most regions, using climatological vertical profiles for the air mass factor calculations do not introduce significant errors. Only during the winter months does applying the US Standard Atmosphere climatological NO_2 profiles result in a slight overestimation of stratospheric AMFs, which can reach up to 4 %. The influence of the temperature dependence of the NO_2 absorption cross section is more substantial. Using a fixed temperature of 243 K in the DOAS fit leads to an overestimation of stratospheric NO_2 abundances by 6.4 % on average. During winter months, the influence can be as large as 15 % in the climatological means.

The present study reveals many details on the interpretation of the involved datasets, which were found to be in very good agreement with each other. In several cases, shortcomings of the reference sector method can be made up for by applying either the limb or the model correction scheme, significantly improving the consistency of the resulting tropospheric columns. For example, we found that during winter, tropospheric columns are underestimated by a factor of 2 over North America when using the reference sector method.

While it is difficult to quantify the error of the resulting tropospheric slant columns, we can conclude that our stratospheric correction scheme, while leading to an increase of the random error component by approximately $\sqrt{2}$, minimises the error due to the zonal variability of stratospheric NO_2 fields. When accounting for a systematic bias between the two stratospheric datasets by forcing their difference to be zero over the Pacific Ocean, SCIAMACHY limb measurements and Oslo CTM2 simulations exhibit very good agreement. Climatological differences between the two vertical column datasets are smaller than 2×10^{14} molec cm^{-2} on an annual basis, and in most cases smaller than 3×10^{14} molec cm^{-2} on a monthly basis. However, the lack of independent measurements and thorough validation makes it impossible to say which of the two datasets is more correct. In most cases, uncertainties of the order of magnitude deduced from the observed differences between the two stratospheric corrections result in tropospheric slant column uncertainties of less than 5×10^{14} molec cm^{-2}, but in some rare cases can be as large as 2.5×10^{15} molec cm^{-2}. While for over polluted regions, the stratospheric contribution to the uncertainties can usually be neglected when applying the limb/nadir matching technique, it has to be considered over clean regions, in particular where the agreement between model and measurement is found to be less sound.

The limb/nadir matching technique described in this study will be tested for implementation as operational SCIAMACHY NO_2 product in the near future. This approach leads to a significant improvement of the stratospheric correction in the retrieval of tropospheric NO_2 abundances from SCIAMACHY measurements. As modelled stratospheric NO_2 columns from the Oslo CTM2 agree very well with the measured quantities after correcting for a systematic bias, they prove to be a feasible stratospheric correction scheme in cases where limb/nadir matching cannot be applied, e.g. with other satellite sensors. It should be noted, however, that the need for offset correction will introduce difficulties when trying to apply model data for the upcoming geostationary satellite missions that have only limited spatial coverage.

Finally, this study shows the importance of measuring stratospheric NO_2 accurately for both the interpretation of total column NO_2 and the derivation of tropospheric NO_2 as proposed for SCIAMACHY, and points out limitations of the nadir-only observations of GOME, GOME-2, OMI, and related instruments. Limb and occultation measurements of NO_2 are needed to complement the nadir observations in order to generate an adequate global observing system.

Supplementary material related to this article is available online at: http://www.atmos-meas-tech.net/6/565/2013/amt-6-565-2013-supplement.pdf.

Acknowledgements. Funding by the Earth System Science Research School (ESSReS), an initiative of the Helmholtz Association of German research centres (HGF) at the Alfred Wegener Institute for Polar and Marine Research, is gratefully acknowledged. The authors further acknowledge funding by the European Union Seventh Framework Programme (FP7/2007-2013) project CityZen (Grant Agreement no. 212095), by the DLR project SADOS (FKZ 50EE0727 and 50EE1105), and by ESA through the SCIAMACHY Quality Working Group. Øivind Hodnebrog has also received funding from the Research Council of Norway (project no. 188134/E10). Thank you to Steffen Beirle for many fruitful discussions. Tropopause heights have been calculated by Stefan Bötel and Felix Ebojie. SCIAMACHY radiances have been provided by ESA. ECMWF meteorological data were supplied by the European Centre for Medium-Range Weather Forecasts at Reading, UK. Some data used in this study were calculated at German HLRN (High-Performance Computer Center North). The authors would like to thank three anonymous reviewers for their comments and suggestions which helped to improve the final version of this manuscript.

The service charges for this open access publication have been partially covered by the Deutsche Forschungsgemeinschaft (DFG).

Edited by: A. J. M. Piters

References

Bauer, R., Rozanov, A., McLinden, C. A., Gordley, L. L., Lotz, W., Russell III, J. M., Walker, K. A., Zawodny, J. M., Ladstätter-Weißenmayer, A., Bovensmann, H., and Burrows, J. P.: Validation of SCIAMACHY limb NO_2 profiles using solar occultation measurements, Atmos. Meas. Tech., 5, 1059–1084, doi:10.5194/amt-5-1059-2012, 2012.

Beirle, S., Platt, U., Wenig, M., and Wagner, T.: NO_x production by lightning estimated with GOME, Adv. Space Res., 34, 793–797, doi:10.1016/j.asr.2003.07.069, 2004.

Beirle, S., Kühl, S., Pukı̄te, J., and Wagner, T.: Retrieval of tropospheric column densities of NO_2 from combined SCIAMACHY nadir/limb measurements, Atmos. Meas. Tech., 3, 283–299, doi:10.5194/amt-3-283-2010, 2010.

Berntsen, T. K. and Isaksen, I. S. A.: A global three-dimensional chemical transport model for the troposphere 1. Model description and CO and ozone results, J. Geophys. Res., 102, 21239–21280, doi:10.1029/97JD01140, 1997.

Bertram, T. H., Heckel, A., Richter, A., Burrows, J. P., and Cohen, R. C.: Satellite measurements of daily variations in soil NO_x emissions, Geophys. Res. Lett., 32, L24812, doi:10.1029/2005GL024640, 2005.

Bian, H. and Prather, M. J.: Fast-J2: accurate simulation of stratospheric photolysis in global chemical models, J. Atmos. Chem., 41, 281–296, doi:10.1023/A:1014980619462, 2002.

Boersma, K. F., Eskes, H. J., and Brinksma, E. J.: Error analysis for tropospheric NO_2 retrieval from space, J. Geophys. Res., 109, D04311, doi:10.1029/2003JD003962, 2004.

Boersma, K. F., Eskes, H. J., Veefkind, J. P., Brinksma, E. J., van der A, R. J., Sneep, M., van den Oord, G. H. J., Levelt, P. F., Stammes, P., Gleason, J. F., and Bucsela, E. J.: Near-real time retrieval of tropospheric NO_2 from OMI, Atmos. Chem. Phys., 7, 2103–2118, doi:10.5194/acp-7-2103-2007, 2007.

Bogumil, K., Orphal, J., Homann, T., Voigt, S., Spietz, P., Fleischmann, O., Vogel, A., Hartmann, M., Kromminga, H., Bovensmann, H., Frerick, J., and Burrows, J.: Measurements of molecular absorption spectra with the SCIAMACHY pre-flight model: instrument characterization and reference data for atmospheric remote-sensing in the 230–2380 nm region, J. Photochem. Photobiol. A, 157, 167–184, doi:10.1016/S1010-6030(03)00062-5, 2003.

Bovensmann, H., Burrows, J. P., Buchwitz, M., Frerick, F., Noël, S., and Rozanov, V. V.: SCIAMACHY: mission objectives and measurement modes, J. Atmos. Sci., 56, 127–150, doi:10.1175/1520-0469(1999)056<0127:SMOAMM>2.0.CO;2, 1999.

Brasseur, G. P. and Solomon, S.: Aeronomy of the Middle Atmosphere, 3rd Edn., Springer, 2005.

Bucsela, E. J., Celarier, E. A., Wenig, M. O., Gleason, J. F., Veefkind, J. P., Boersma, K. F., and Brinksma, E. J.: Algorithm for NO_2 vertical column retrieval from the ozone monitoring instrument, IEEE T. Geosci. Remote, 44, 1245–1258, doi:10.1109/TGRS.2005.863715, 2006.

Burrows, J., Hölzle, E., Goede, A., Visser, H., and Fricke, W.: SCIAMACHY – scanning imaging absorption spectrometer for atmospheric chartography, Acta Astronaut., 35, 445–451, doi:10.1016/0094-5765(94)00278-T, 1995.

Burrows, J. P., Dehn, A., Deters, B., Himmelmann, S., Richter, A., Voigt, S., and Orphal, J.: Atmospheric remote-sensing reference data from GOME: Part 1. Temperature-dependent absorption cross-sections of NO_2 in the 231–794 nm range, J. Quant. Spectrosc. Ra., 60, 1025–1031, doi:10.1016/S0022-4073(97)00197-0, 1998.

Burrows, J. P., Weber, M., Buchwitz, M., Rozanov, V. V., Ladstaetter-Weissenmayer, A., Richter, A., DeBeek, R., Hoogen, R., Bramstedt, K., Eichmann, K., and Eisinger, M.: The global ozone monitoring experiment (GOME): mission concept and first scientific results, J. Atmos. Sci., 56, 151–175, doi:10.1175/1520-0469(1999)056<0151:TGOMEG>2.0.CO;2, 1999.

Burrows, J. P., Platt, U., and Borrell, P.: The Remote Sensing of Tropospheric Composition from Space, 1st Edn., Springer, 2011.

Callies, J., Corpaccioli, E., Eisinger, M., Hahne, A., and Lefebvre, A.: GOME-2 – Metop's second-generation sensor for operational ozone monitoring, ESA Bull., 102, 28–36, 2000.

Chance, K.: Analysis of BrO measurements from the global ozone monitoring experiment, Geophys. Res. Lett., 25, 3335–3338, doi:10.1029/98GL52359, 1998.

Committee on Extension to the Standard Atmosphere: US Standard Atmosphere, 1976, US Government Printing Office, Washington, D.C., 1976.

Crutzen, P. J.: The role of NO and NO_2 in the chemistry of the troposphere and stratosphere, Ann. Rev. Earth Planet. Sci., 7, 443–472, 1doi:0.1146/annurev.ea.07.050179.002303, 1979.

de Smedt, I., Stavrakou, T., Müller, J., von der A, R. J., and van Roozendael, M.: Trend detection in satellite observations of formaldehyde tropospheric columns, Geophys. Res. Lett., 37, L18808, doi:10.1029/2010GL044245, 2010.

Dee, D. P., Uppala, S. M., Simmons, A. J., Berrisford, P., Poli, P., Kobayashi, S., Andrae, U., Balmaseda, M. A., Balsamo, G., Bauer, P., Bechtold, P., Beljaars, A. C. M., van de Berg, L., Bidlot, J., Bormann, N., Delsol, C., Dragani, R., Fuentes, M., Geer, A. J., Haimberger, L., Healy, S. B., Hersbach, H., Hólm, E. V., Isaksen, L., Kållberg, P., Köhler, M., Matricardi, M., McNally, A. P., Monge-Sanz, B. M., Morcrette, J., Park, B., Peubey, C., de Rosnay, P., Tavolato, C., Thépaut, J., and Vitart, F.: The ERA-Interim reanalysis: configuration and performance of the data assimilation system, Q. J. Roy. Meteorol. Soc., 137, 553–597, doi:10.1002/qj.828, 2011.

Dirksen, R. J., Boersma, K. F., Eskes, H. J., Ionov, D. V., Bucsela, E. J., Levelt, P. F., and Kelder, H. M.: Evaluation of stratospheric NO_2 retrieved from the ozone monitoring instrument: intercomparison, diurnal cycle, and trending, J. Geophys. Res., 116, D08305, doi:10.1029/2010JD014943, 2011.

Ebojie, F., von Savigny, C., Ladstätter-Weißenmayer, A., Rozanov, A., Weber, M., Eichmann, K., Bötel, S., Rahpoe, N., Bovensmann, H., and Burrows, J. P.: Seasonal variability of tropospheric ozone derived from SCIAMACHY limb-nadir matching observations, in preparation, 2013.

Elbern, H., Hendricks, J, and Ebel, A.:A Climatology of Tropopause Folds by Global Analyses, Theor. Appl. Climatol., 59, 3, 181–200, doi:10.1007/s007040050023, 1998.

Gottwald, M. and Bovensmann, H. (Eds.): SCIAMACHY – Exploring the Changing Earth's Atmosphere, Springer Netherlands, Dordrecht, 2011.

Granier, C., Lamarque, J., Mieville, A., Müller, J., Olivier, J., Orlando, J., Peters, J., Petron, G., Tyndall, G., and Wallens, S.: POET, a database of surface emissions of ozone precursors, available at: http://www.aero.jussieu.fr/projet/ACCENT/POET.php (last access: 11 June 2012), 2005.

Granier, C., Bessagnet, B., Bond, T., D'Angiola, A., Denier van der Gon, H., Frost, G. J., Heil, A., Kaiser, J. W., Kinne, S., Klimont, Z., Kloster, S., Lamarque, J., Liousse, C., Masui, T., Meleux, F., Mieville, A., Ohara, T., Raut, J., Riahi, K., Schultz, M. G., Smith, S. J., Thompson, A., Aardenne, J., Werf, G. R., and Vuuren, D. P.: Evolution of anthropogenic and biomass burning emissions of air pollutants at global and regional scales during the 1980–2010 period, Climatic Change, 109, 163–190, doi:10.1007/s10584-011-0154-1, 2011.

Heckel, A., Kim, S.-W., Frost, G. J., Richter, A., Trainer, M., and Burrows, J. P.: Influence of low spatial resolution a priori data on tropospheric NO_2 satellite retrievals, Atmos. Meas. Tech., 4, 1805–1820, doi:10.5194/amt-4-1805-2011, 2011.

Hesstvedt, E., Hov, Ö., and Isaksen, I. S. A.: Quasi-steady-state approximations in air pollution modeling: comparison of two numerical schemes for oxidant prediction, Int. J. Chem. Kinet., 10, 971–994, doi:10.1002/kin.550100907, 1978.

Heue, K.-P., Richter, A., Bruns, M., Burrows, J. P., v. Friedeburg, C., Platt, U., Pundt, I., Wang, P., and Wagner, T.: Validation of SCIAMACHY tropospheric NO_2-columns with AMAXDOAS measurements, Atmos. Chem. Phys., 5, 1039–1051, doi:10.5194/acp-5-1039-2005, 2005.

Hoinka, K. P.: Statistics of the global tropopause pressure, Mon. Weather Rev., 126, 3303–3325, doi:10.1175/1520-0493(1998)126<3303:SOTGTP>2.0.CO;2, 1998.

Holtslag, A. A. M., De Bruijn, E. I. F., and Pan, H.: A high resolution air mass transformation model for short-range weather forecasting, Mon. Weather Rev., 118, 1561–1575, doi:10.1175/1520-0493(1990)118<1561:AHRAMT>2.0.CO;2, 1990.

Lee, D. S., Köhler, I., Grobler, E., Rohrer, F., Sausen, R., Gallardo-Klenner, L., Olivier, J. G. J., Dentener, F. J., and Bouwman, A. F.: Estimations of global NO_x emissions and their uncertainties, Atmos. Environ., 31, 1735–1749, doi:10.1016/S1352-2310(96)00327-5, 1997.

Leitão, J., Richter, A., Vrekoussis, M., Kokhanovsky, A., Zhang, Q. J., Beekmann, M., and Burrows, J. P.: On the improvement of NO_2 satellite retrievals – aerosol impact on the airmass factors, Atmos. Meas. Tech., 3, 475–493, doi:10.5194/amt-3-475-2010, 2010.

Lerot, C., Stavrakou, T., De Smedt, I., Müller, J., and Van Roozendael, M.: Glyoxal vertical columns from GOME-2 backscattered light measurements and comparisons with a global model, Atmos. Chem. Phys., 10, 12059–12072, doi:10.5194/acp-10-12059-2010, 2010.

Leue, C., Wenig, M., Wagner, T., Klimm, O., Platt, U., and Jähne, B.: Quantitative analysis of NO_x emissions from Global Ozone Monitoring Experiment satellite image sequences, J. Geophys. Res., 106, 5493–5505, doi:10.1029/2000JD900572, 2001.

Levelt, P., van den Oord, G., Dobber, M., Malkki, A., Visser, H., de Vries, J., Stammes, P., Lundell, J., and Saari, H.: The ozone monitoring instrument, IEEE T. Geosci. Remote, 44, 1093–1101, doi:10.1109/TGRS.2006.872333, 2006.

Martin, R. V., Chance, K., Jacob, D. J., Kurosu, T. P., Spurr, R. J. D., Bucsela, E., Gleason, J. F., Palmer, P. I., Bey, I., Fiore, A. M., Li, Q., Yantosca, R. M., and Koelemeijer, R. B. A.: An improved retrieval of tropospheric nitrogen dioxide from GOME, J. Geophys. Res., 107, 4437, doi:10.1029/2001JD001027, 2002.

Nüß, J. H.: Improvements of the retrieval of tropospheric NO_2 from GOME and SCIAMACHY data, PhD Thesis, University of Bremen, 2005.

Nüß, H., Richter, A., Valks, P., and Burrows, J. P.: Improvements of the NO_2 Total Column Retrieval for GOME-2, O3M SAF Visiting Scientist Activity, Final Report, Universität Bremen, 2006.

Platt, U. and Stutz, J.: Differential Optical Absorption Spectroscopy, Physics of Earth and Space Environments, Springer, Berlin, 2008.

Platt, U. and Wagner, T.: Satellite mapping of enhanced BrO concentrations in the troposphere, Nature, 395, 486–490, doi:10.1038/26723, 1998.

Prather, M. J.: Numerical advection by conservation of second-order moments, J. Geophys. Res., 91, 6671–6681, doi:10.1029/JD091iD06p06671, 1986.

Price, C., Penner, J., and Prather, M.: NO_x from lightning 1. Global distribution based on lightning physics, J. Geophys. Res., 102, 5929–5941, doi:10.1029/96JD03504, 1997.

Pukïte, J., Kühl, S., Deutschmann, T., Dörner, S., Jöckel, P., Platt, U., and Wagner, T.: The effect of horizontal gradients and spatial measurement resolution on the retrieval of global vertical NO_2 distributions from SCIAMACHY measurements in limb only mode, Atmos. Meas. Tech., 3, 1155–1174, doi:10.5194/amt-3-1155-2010, 2010.

Richter, A. and Burrows, J. P.: Tropospheric NO_2 from GOME measurements, Adv. Space Res., 29, 1673–1683, doi:10.1016/S0273-1177(02)00100-X, 2002.

Richter, A., Wittrock, F., Eisinger, M., and Burrows, J. P.: GOME observations of tropospheric BrO in northern hemispheric spring and summer 1997, Geophys. Res. Lett., 25, 2683–2686, doi:10.1029/98GL52016, 1998.

Richter, A., DeBeek, R., Fietkau, S., Heckel, A., Löwe, A. G., Medeke, T., Oetjen, H., Weber, M., Wittrock, F., and Burrows, J. P.: Validation von SCIAMACHY level-2 Daten mit bodengebundenen DOAS-Messungen, Tech. Rep., Bremen, 2004.

Richter, A., Burrows, J. P., Nüß, H., Granier, C., and Niemeier, U.: Increase in tropospheric nitrogen dioxide over China observed from space, Nature, 437, 129–132, doi:10.1038/nature04092, 2005.

Richter, A., Begoin, M., Hilboll, A., and Burrows, J. P.: An improved NO_2 retrieval for the GOME-2 satellite instrument, Atmos. Meas. Tech., 4, 1147–1159, doi:10.5194/amt-4-1147-2011, 2011.

Rozanov, A., Bovensmann, H., Bracher, A., Hrechanyy, S., Rozanov, V. V., Sinnhuber, M., Stroh, F., and Burrows, J. P.: NO_2 and BrO vertical profile retrieval from SCIAMACHY limb measurements: sensitivity studies, Adv. Space Res., 36, 846–854, doi:10.1016/j.asr.2005.03.013, 2005a.

Rozanov, A., Rozanov, V. V., Buchwitz, M., Kokhanovsky, A. A., and Burrows, J. P.: SCIATRAN 2.0 – A new radiative transfer model for geophysical applications in the 175-2400 nm spectral region, Adv. Space Res., 36, 1015–1019, doi:10.1016/j.asr.2005.03.012, 2005b.

Schönhardt, A., Richter, A., Wittrock, F., Kirk, H., Oetjen, H., Roscoe, H. K., and Burrows, J. P.: Observations of iodine monoxide columns from satellite, Atmos. Chem. Phys., 8, 637–653, doi:10.5194/acp-8-637-2008, 2008.

Schultz, M. G., Heil, A., Hoelzemann, J. J., Spessa, A., Thonicke, K., Goldammer, J. G., Held, A. C., Pereira, J. M. C., and Bolscher, M. v. h.: Global wildland fire emissions from 1960 to 2000, Global Biogeochem. Cy., 22, GB2002, doi:10.1029/2007GB003031, 2008.

Sierk, B., Richter, A., Rozanov, A., von Savigny, C., Schmoltner, A. M., Buchwitz, M., Bovensmann, H., and Burrows, J. P.: Retrieval and monitoring of atmospheric trace gas concentrations in nadir and limb geometry using the space-borne Sciamachy instrument, Environ. Monit. Assess., 120, 65–77, doi:10.1007/s10661-005-9049-9, 2006.

Sioris, C. E., Kurosu, T. P., Martin, R. V., and Chance, K.: Stratospheric and tropospheric NO_2 observed by SCIAMACHY: first results, Adv. Space Res., 34, 780–785, doi:10.1016/j.asr.2003.08.066, 2004.

Sprenger, M. and Wernli, H.: A northern hemispheric climatology of cross-tropopause exchange for the ERA15 time period (1979–1993), J. Geophys. Res., 108, 8521, doi:10.1029/2002JD002636, 2003.

Stordal, F., Isaksen, I. S. A., and Horntveth, K.: A diabatic circulation two-dimensional model with photochemistry: simulations of ozone and long-lived tracers with surface sources, J. Geophys. Res., 90, 5757–5776, doi:10.1029/JD090iD03p05757, 1985.

Søvde, O. A., Gauss, M., Smyshlyaev, S. P., and Isaksen, I. S. A.: Evaluation of the chemical transport model Oslo CTM2 with focus on arctic winter ozone depletion, J. Geophys. Res., 113, D09304, doi:10.1029/2007JD009240, 2008.

Tiedtke, M.: A comprehensive mass flux scheme for cumulus parameterization in large-scale models, Mon.

Weather Rev., 117, 1779–1800, doi:10.1175/1520-0493(1989)117<1779:ACMFSF>2.0.CO;2, 1989.

van der Werf, G. R., Randerson, J. T., Giglio, L., Collatz, G. J., Kasibhatla, P. S., and Arellano Jr., A. F.: Interannual variability in global biomass burning emissions from 1997 to 2004, Atmos. Chem. Phys., 6, 3423–3441, doi:10.5194/acp-6-3423-2006, 2006.

Vountas, M., Rozanov, V. V., and Burrows, J. P.: Ring effect: impact of rotational Raman scattering on radiative transfer in Earth's atmosphere, J. Quant. Spectrosc. Ra., 60, 943–961, doi:10.1016/S0022-4073(97)00186-6, 1998.

Vountas, M., Richter, A., Wittrock, F., and Burrows, J. P.: Inelastic scattering in ocean water and its impact on trace gas retrievals from satellite data, Atmos. Chem. Phys., 3, 1365–1375, doi:10.5194/acp-3-1365-2003, 2003.

Wang, P., Stammes, P., van der A, R., Pinardi, G., and van Roozendael, M.: FRESCO+: an improved O_2 A-band cloud retrieval algorithm for tropospheric trace gas retrievals, Atmos. Chem. Phys., 8, 6565–6576, doi:10.5194/acp-8-6565-2008, 2008.

Wenig, M., Kühl, S., Beirle, S., Bucsela, E., Jähne, B., Platt, U., Gleason, J., and Wagner, T.: Retrieval and analysis of stratospheric NO_2 from the global ozone monitoring experiment, J. Geophys. Res., 109, D04315, doi:10.1029/2003JD003652, 2004.

Wild, O., Zhu, X., and Prather, M. J.: Fast-J: accurate simulation of in- and below-cloud photolysis in tropospheric chemical models, J. Atmos. Chem., 37, 245–282, doi:10.1023/A:1006415919030, 2000.

Williams, E. J., Hutchinson, G. L., and Fehsenfeld, F. C.: NO_x and N_2O emissions from soil, Global Biogeochem. Cy., 6, 351–388, doi:10.1029/92GB02124, 1992.

Wittrock, F.: The retrieval of oxygenated volatile organic compounds by remote sensing techniques, Ph.D. thesis, Universität Bremen, http://nbn-resolving.de/urn:nbn:de:gbv:46-diss000104818 (last access: 11 June 2012), 2006.

Zahn, M., and von Storch, H.: A long-term climatology of North Atlantic polar lows, Geophys. Res. Lett., 35, L22702, doi:10.1029/2008GL035769, 2008.